Innovation, Sciences et Développement économique Canada
Office de la Propriété Intellectuelle du Canada

Innovation, Science and Economic Development Canada
Canadian Intellectual Property Office

CA 2930872 C 2022/05/31

(11)(21) 2 930 872

(12) BREVET CANADIEN
CANADIAN PATENT

(13) C

(86) Date de dépôt PCT/PCT Filing Date: 2014/11/25
(87) Date publication PCT/PCT Publication Date: 2015/06/04
(45) Date de délivrance/Issue Date: 2022/05/31
(85) Entrée phase nationale/National Entry: 2016/05/16
(86) N° demande PCT/PCT Application No.: US 2014/067415
(87) N° publication PCT/PCT Publication No.: 2015/081101
(30) Priorité/Priority: 2013/11/26 (US61/908,861)

(51) Cl.Int./Int.Cl. *C12N 15/85* (2006.01), *A61K 48/00* (2006.01), *A61P 3/00* (2006.01), *C12N 15/55* (2006.01), *C12N 15/86* (2006.01), *C12N 15/864* (2006.01), *C12N 5/10* (2006.01), *C12N 9/16* (2006.01)

(72) Inventeurs/Inventors:
CHOU, JANICE J., US;
BYRNE, BARRY J., US

(73) Propriétaires/Owners:
UNIVERSITY OF FLORIDA RESEARCH FOUNDATION, INCORPORATED, US;

(54) Titre : VECTEURS DE TYPE VIRUS ADENO-ASSOCIE POUR LE TRAITEMENT DE MALADIE DU STOCKAGE DU GLYCOGENE

(54) Title: ADENO-ASSOCIATED VIRUS VECTORS FOR TREATMENT OF GLYCOGEN STORAGE DISEASE

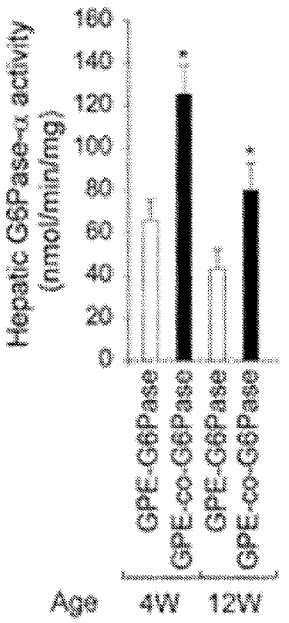

(57) Abrégé/Abstract:
The present disclosure describes improved adeno-associated virus (AAV) vectors for gene therapy applications in the treatment of glycogen storage disease, particularly glycogen storage disease type Ia (GSD-Ia). Described are recombinant nucleic acid molecules, vectors and recombinant AAV that include a G6PC promoter/enhancer, a synthetic intron, a G6PC coding sequence (such as a wild-type or codon-optimized G6PC coding sequence), and stuffer nucleic acid sequence situated between the G6PC promoter/enhancer and the intron, as well as between the intron and the G6PC coding sequence. The recombinant AAVs disclosed herein exhibit highly efficient liver transduction and are capable of correcting metabolic abnormalities in an animal model of GSD-Ia.

(11)(21) 2 930 872

(13) C

(73) Propriétaires(suite)/Owners(continued):
THE UNITED STATES OF AMERICA, AS REPRESENTED BY THE SECRETARY, DEPARTMENT OF HEALTH AND HUMAN SERVICES, US

(74) Agent: SMART & BIGGAR LLP

(12) INTERNATIONAL APPLICATION PUBLISHED UNDER THE PATENT COOPERATION TREATY (PCT)

(19) World Intellectual Property Organization
International Bureau

(43) International Publication Date
4 June 2015 (04.06.2015)

WIPO | PCT

(10) International Publication Number
WO 2015/081101 A1

(51) International Patent Classification:
C12N 9/16 (2006.01) *C12N 15/86* (2006.01)
A61K 48/00 (2006.01)

(21) International Application Number:
PCT/US2014/067415

(22) International Filing Date:
25 November 2014 (25.11.2014)

(25) Filing Language: English

(26) Publication Language: English

(30) Priority Data:
61/908,861 26 November 2013 (26.11.2013) US

(71) Applicants: **THE UNITED STATES OF AMERICA, AS REPRESENTED BY THE SECRETARY DEPARTMENT OF HEALTH AND HUMAN SERVICES** [US/US]; National Institutes of Health, Office of Technology Transfer, 6011 Executive Boulevard, Suite 325, MSC 7660, Bethesda, MD 20892-7660 (US). **UNIVERSITY OF FLORIDA RESEARCH FOUNDATION, INCORPORATED** [US/US]; 223 Grinter Hall, Gainesville, FL 32611 (US).

(72) Inventors: **CHOU, Janice, J.**; NIH/NICHD, Building 10, Room 9D42, Bethesda, MD 20892 (US). **BYRNE, Barry, J.**; University of Florida, Child Health Research Institute, PO Box 100296, Gainesville, FL 32610-0296 (US).

(74) Agent: **CONNOLLY, Jodi, L.**; Klarquist Sparkman, LLP, One World Trade Center, Suite 1600, 121 SW Salmon Street, Portland, OR 97204 (US).

(81) Designated States *(unless otherwise indicated, for every kind of national protection available)*: AE, AG, AL, AM, AO, AT, AU, AZ, BA, BB, BG, BH, BN, BR, BW, BY, BZ, CA, CH, CL, CN, CO, CR, CU, CZ, DE, DK, DM, DO, DZ, EC, EE, EG, ES, FI, GB, GD, GE, GH, GM, GT, HN, HR, HU, ID, IL, IN, IR, IS, JP, KE, KG, KN, KP, KR, KZ, LA, LC, LK, LR, LS, LU, LY, MA, MD, ME, MG, MK, MN, MW, MX, MY, MZ, NA, NG, NI, NO, NZ, OM, PA, PE, PG, PH, PL, PT, QA, RO, RS, RU, RW, SA, SC, SD, SE, SG, SK, SL, SM, ST, SV, SY, TH, TJ, TM, TN, TR, TT, TZ, UA, UG, US, UZ, VC, VN, ZA, ZM, ZW.

[Continued on next page]

(54) Title: ADENO-ASSOCIATED VIRUS VECTORS FOR TREATMENT OF GLYCOGEN STORAGE DISEASE

(57) Abstract: The present disclosure describes improved adeno-associated virus (AAV) vectors for gene therapy applications in the treatment of glycogen storage disease, particularly glycogen storage disease type Ia (GSD-Ia). Described are recombinant nucleic acid molecules, vectors and recombinant AAV that include a G6PC promoter/enhancer, a synthetic intron, a G6PC coding sequence (such as a wild-type or codon-optimized G6PC coding sequence), and stuffer nucleic acid sequence situated between the G6PC promoter/enhancer and the intron, as well as between the intron and the G6PC coding sequence. The recombinant AAVs disclosed herein exhibit highly efficient liver transduction and are capable of correcting metabolic abnormalities in an animal model of GSD-Ia.

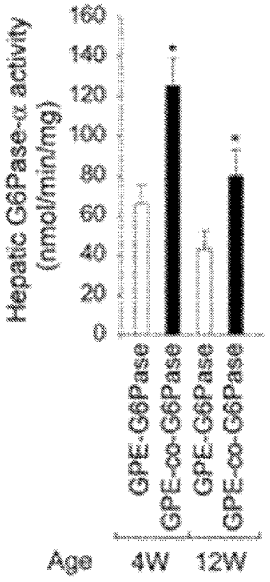

FIG. 11

WO 2015/081101 A1

WO 2015/081101 A1

(84) Designated States *(unless otherwise indicated, for every kind of regional protection available)*: ARIPO (BW, GH, GM, KE, LR, LS, MW, MZ, NA, RW, SD, SL, ST, SZ, TZ, UG, ZM, ZW), Eurasian (AM, AZ, BY, KG, KZ, RU, TJ, TM), European (AL, AT, BE, BG, CH, CY, CZ, DE, DK, EE, ES, FI, FR, GB, GR, HR, HU, IE, IS, IT, LT, LU, LV, MC, MK, MT, NL, NO, PL, PT, RO, RS, SE, SI, SK, SM, TR), OAPI (BF, BJ, CF, CG, CI, CM, GA, GN, GQ, GW, KM, ML, MR, NE, SN, TD, TG).

Declarations under Rule 4.17:

— *of inventorship (Rule 4.17(iv))*

Published:

— *with international search report (Art. 21(3))*

— *with sequence listing part of description (Rule 5.2(a))*

ADENO-ASSOCIATED VIRUS VECTORS FOR TREATMENT OF GLYCOGEN STORAGE DISEASE

CROSS REFERENCE TO RELATED APPLICATIONS

This application claims the benefit of U.S. Provisional Application No. 61/908,861, filed November 26, 2013.

FIELD

This disclosure concerns gene therapy vectors for the treatment of glycogen storage disease, particularly glycogen storage disease type Ia.

BACKGROUND

Glycogen storage disease type Ia (GSD-Ia or von Gierke disease, MIM232200) is caused by a deficiency in glucose-6-phosphatase-α (G6Pase-α), an enzyme that is expressed primarily in the liver, kidney, and intestine (Chou *et al.*, *Nat Rev Endocrinol* 6:676-688, 2010). G6Pase-α, encoded by the *G6PC* gene, is a hydrophobic protein anchored in the endoplasmic reticulum (ER) by nine transmembrane helices (Chou *et al.*, *Nat Rev Endocrinol* 6:676-688, 2010). This enzyme catalyzes the hydrolysis of glucose-6-phosphate (G6P) to glucose and phosphate in the terminal step of glycogenolysis and gluconeogenesis. Patients affected by GSD-Ia are unable to maintain glucose homeostasis and present with fasting hypoglycemia, growth retardation, hepatomegaly, nephromegaly, hyperlipidemia, hyperuricemia, and lactic academia (Chou *et al.*, *Nat Rev Endocrinol* 6:676-688, 2010).

There is currently no cure for GSD-Ia. Hypoglycemia can be managed using dietary therapies (Greene *et al.*, *N Engl J Med* 294:423-425, 1976; Chen *et al.*, *N Engl J Med* 310:171-175, 1984) that enable patients to attain near normal growth and pubertal development. However, the longer term clinical complications, and their underlying pathological processes, remain uncorrected. One of the most significant chronic risks is hepatocellular adenoma (HCA), that develops in 70-80% of GSD-I patients over 25 years old (Chou *et al.*, *Nat Rev Endocrinol* 6:676-688, 2010; Labrune *et al.*, *J Pediatr Gastroenterol Nutr* 24:276-279 , 1997; Rake *et al.*, *Eur J Pediatr* 161(Suppl 1):S20-S34, 2002). HCAs in GSD-Ia patients are small, multiple, and nonencapsulated, with complications including local compression and intratumoral hemorrhage. In 10% of GSD-Ia patients, HCAs undergo malignant transformation to hepatocellular carcinoma (HCC) (Chou *et al.*, *Nat Rev Endocrinol* 6:676-688, 2010; Rake *et al.*, *Eur J Pediatr* 161(Suppl 1):S20-S34, 2002; Franco *et al.*, *J Inherit Metab Dis* 28:153-162, 2005).

Date Reçue/Date Received 2021-04-06

Gene therapy studies using recombinant adeno-associated virus (AAV) carrying G6Pase-α have been performed in animal models of GSD-Ia; these studies have demonstrated efficacy in the absence of toxicity (reviewed in Chou and Mansfield, *Expert Opin Biol Ther* 11:1011-1024, 2011). Previous studies using the mouse model of GSD-Ia have shown that recombinant AAV expressing G6Pase-α directed by the CBA promoter/CMV enhancer (Ghosh *et al.*, *Gene Ther* 13:321-329, 2006), the canine *G6PC* promoter (Koeberl *et al.*, *Gene Ther* 13:1281-1289, 2006), or the human *G6PC* promoter at nucleotides -298 to +128 of the *G6PC* 5' flanking region (Koeberl *et al.*, *Mol Ther* 16:665-672, 2008) deliver the G6Pase-α transgene to the liver and achieve extended correction of this disorder. However, while these studies have shown promise, none have been capable of completely correcting hepatic G6Pase-α deficiency.

SUMMARY

Provided herein are recombinant nucleic acid molecules, adeno-associated virus (AAV) vectors and recombinant AAV that can be used in gene therapy applications for the treatment of glycogen storage disease, specifically GSD-Ia.

In some embodiments, the recombinant nucleic acid molecules include a G6PC promoter/enhancer, a synthetic intron, and the G6PC coding region, the latter optionally being codon-optimized for expression in human cells. The recombinant nucleic acid molecules further include stuffer nucleic acid sequence situated between the G6PC promoter/enhancer and the intron, as well as between the intron and the G6PC coding sequence. In particular non-limiting examples, the recombinant nucleic acid molecules comprise nucleotides 182-4441 of SEQ ID NO: 1 or nucleotides 182-4441 of SEQ ID NO: 3.

In some embodiments, the recombinant nucleic acid molecules further include 5' and 3' inverted terminal repeat (ITR) sequences. In some examples, the recombine ant nucleic acid molecules comprise nucleotides 17-4819 of SEQ ID NO: 1 or nucleotides 17-4819 of SEQ ID NO: 3. In other embodiments, the recombinant nucleic acid molecules comprise the complete vector nucleic acid sequences of SEQ ID NO: 1 or SEQ ID NO: 3.

Also provided are vectors comprising the recombinant nucleic acid molecules disclosed herein. In some embodiments, the vectors are AAV vectors, such as AAV8 vectors. Further provided are isolated host cells comprising the recombinant nucleic acid molecules or vectors disclosed herein. For example, the isolated host cells can be cells suitable for propagation of AAV.

Also provided herein are recombinant AAV (rAAV) comprising the recombinant nucleic acid molecules disclosed herein. Compositions comprising the rAAV are also provided by the present disclosure.

Further provided is a method of treating a subject diagnosed with a glycogen storage disease, comprising selecting a subject with glycogen storage disease type Ia (GSD-Ia) and administering to the subject a therapeutically effective amount of the rAAV, or compositions comprising the rAAV, disclosed herein.

Further provided is use of a therapeutically effective amount of the rAAV as described herein, or the composition as described herein, for treating a subject diagnosed with a glycogen storage disease.

The foregoing and other objects, features, and advantages of the invention will become more apparent from the following detailed description, which proceeds with reference to the accompanying figures.

BRIEF DESCRIPTION OF THE DRAWINGS

FIGS. 1A-1B are graphs showing the results of phenotype analysis of AAV-GPE-infused *G6pc*$^{-/-}$ mice. (FIG. 1A) Body weights of female *G6pc*$^{-/-}$ mice infused with 1.2 x 10^{11} vg/mouse of AAV-GPE and their female *G6pc*$^{+/+}$/*G6pc*$^{+/-}$ littermates are shown. The age at infusion (2 days, 2 weeks or 4 weeks) is shown above the graph. (○), *G6pc*$^{+/+}$/*G6pc*$^{+/-}$ mice; (●), AAV-GPE-infused *G6pc*$^{-/-}$ mice. (FIG. 1B) Blood glucose, cholesterol, triglyceride, uric acid, and lactic acid levels of mice infused with AAV-GPE are shown. Because of the similarities of the respective metabolites in each group, data shown are pooled data of age 6-24 weeks. (+/+ & +/-), *G6pc*$^{+/+}$/*G6pc*$^{+/-}$, (-/-), *G6pc*$^{-/-}$, or (-/- GPE), *G6pc*$^{-/-}$ mice infused with AAV-GPE at age 2 days (n = 36), 2 weeks (n = 24), or 4 weeks (n = 9). Data are presented as mean ± SEM. $*p < 0.05$, $**p < 0.005$.

FIGS. 2A-2B are graphs showing hepatic G6Pase-α activity and mRNA expression in wild type and AAV-GPE-treated G6pc$^{-/-}$ mice following a 24-hour fast. Seven 2-week, 11 four-week, one 15-week (*) and one 30-week (**) old G6pc$^{-/-}$ mice were infused with varying doses of AAV-GPE; G6Pase-α activity and mRNA expression were evaluated when mice were 70-90 weeks of age. (FIG. 2A) Hepatic G6Pase-α activity is shown at the indicated ages in weeks (W). The mice are grouped based on their G6Pase-α activity relative to wild type activity as low (AAV-L), medium (AAV-M) and high (AAV-H). (FIG. 2B) Hepatic G6Pase-α mRNA expression and its relationship to G6Pase-α activity in AAV-GPE-treated G6pc$^{-/-}$ mice. Data are presented as mean ± SEM. In FIG. 2B, $*P < 0.05$, $**P < 0.005$.

FIGS. 3A-3C are graphs showing the results of phenotype analysis of AAV-GPE-treated G6pc$^{-/-}$ mice at age 70 to 90 weeks. (FIG. 3A) Blood glucose, cholesterol, triglyceride, uric acid, and lactic acid levels. (FIG. 3B) Body weight, body length, and BMI. F, females; M, males.

Date Reçue/Date Received 2021-04-06

(FIG. 3C) Liver weight. Treatments are indicated as: (+/+), wild type mice; (-/- AAV), G6pc$^{-/-}$ mice infused with various dosages of AAV-GPE. AAV-L (n = 6), AAV-M (n = 9), and AAV-H (n = 5) are AAV-GPE-treated G6pc$^{-/-}$ mice expressing 3-9% (low, L), 22-63% (medium, M), and 81-128% (high, H) normal hepatic G6Pase-α activity, respectively. Data are presented as mean ± SEM. $*P < 0.05$, $**P < 0.005$.

FIGS. 4A-4C are graphs showing fasting blood glucose and glucose tolerance profiles. (FIG. 4A) Fasting blood glucose profiles in wild type and AAV-GPE-treated G6pc$^{-/-}$ mice at age 70 to 90 weeks. (FIG. 4B) Fasting blood glucose profiles in untreated G6pc$^{-/-}$ mice at age 6-8 weeks. (FIG. 4C) Glucose tolerance profiles in wild type and AAV-GPE-treated G6pc$^{-/-}$ mice at age 70 to 90 weeks. Wild type or AAV-GPE-infused G6pc$^{-/-}$ mice were fasted for 6 hours, injected intraperitoneally with 2 mg/g of dextrose, and then sampled for blood every 30 minutes via the tail vein. Data are presented as mean ± SEM. (+/+), wild type mice; (-/-), untreated G6pc$^{-/-}$ mice. AAV-L (n = 6), AAV-M (n = 9), and AAV-H (n = 5) are AAV-GPE-treated G6pc$^{-/-}$ mice expression 3-9%, 22-63%, and 81-129% normal hepatic G6Pase-α activity, respectively.

FIGS. 5A-5C are graphs showing blood insulin and hepatic mRNA levels for SREBP-1c and glucokinase in 70 to 90 week-old wild type and AAV-GPE-treated G6pc$^{-/-}$ mice after 24 hours of fast. (FIG. 5A) Fasting blood insulin levels and their relationship to body weights of the animals. (FIG. 5B) Quantification of SREBP-1c mRNA by real-time RT-PCR. (FIG. 5C) Quantification of glucokinase mRNA and the relationship of fasting blood insulin to hepatic glucokinase mRNA levels. (+/+, ○), wild type mice (n = 20); (-/- AAV, ●) AAV-GPE-treated G6pc$^{-/-}$ mice (n = 20). Data are presented as mean ± SEM. $**P< 0.005$.

FIGS. 6A-6D are graphs showing the results of biochemical analyses in 12-week-old wild type, rAAV-GPE- and rAAV-miGPE-treated *G6pc-/-* mice. rAAV-GPE and rAAV-miGPE are rAAV vectors expressing human G6Pase directed by the 2864-bp of the human *G6PC* promoter/enhancer (GPE) and the 382-bp minimal human *G6PC* promoter/enhancer (miGPE), respectively. (FIG. 6A) Hepatic microsomal G6Pase-α activity and its relationship to vector genome copy numbers. (FIG. 6B) Growth curve. (FIG. 6C) BMI values. (FIG. 6D) Blood glucose levels. GPE-high, high dose rAAV-GPE-treated (○); miGPE-high, high dose rAAV-miGPE-treated (●); GPE-low, low dose rAAV-GPE-treated (□); miGPE-low, low dose rAAV-miGPE-treated (■) *G6pc-/-* mice; (+/+), wild type (▼) mice. Data are mean ± SEM. $*P < 0.05$.

FIGS. 7A-7C are graphs showing the results of phenotypic analyses in 12-week-old wild type, rAAV-GPE- and rAAV-miGPE-treated *G6pc-/-* mice. (FIG. 7A) Liver weight. (FIG. 7B) Hepatic glycogen contents. (FIG. 7C) Hepatic triglyceride contents. GPE-high (n = 6), high dose rAAV-GPE-treated; miGPE-high (n = 6), high dose rAAV-miGPE-treated; GPE-low (n = 6),

low dose rAAV-GPE-treated; miGPE-low (n = 6), low dose rAAV-miGPE-treated *G6pc-/-* mice; (+/+), wild type mice. Data are mean ± SEM. $*P < 0.05$.

FIGS. 8A-8C are graphs showing fasting blood glucose and glucose tolerance profiles in 12-week-old wild type, rAAV-GPE- and rAAV-miGPE-treated *G6pc-/-* mice. (FIG. 8A) Fasting blood glucose profiles. (FIG. 8B) Blood glucose levels following a 24-hour fast. (FIG. 8C) Glucose tolerance profiles. GPE-high (n = 6), high dose rAAV-GPE-treated (○); miGPE-high (n = 6), high dose rAAV-miGPE-treated (●); GPE-low (n = 6), low dose rAAV-GPE-treated (□); miGPE-low (n = 6), low dose rAAV-miGPE-treated (■) *G6pc-/-* mice; (+/+), wild type mice (n = 24) (▼). Data are mean ± SEM. $*P < 0.05$, $**P < 0.005$.

FIG. 9 is an alignment of the canine (SEQ ID NO: 10) and human (SEQ ID NO: 4) G6Pase-α protein sequences.

FIG. 10 is a table showing the amino acid differences between human, mouse, rat and canine G6Pase-α.

FIG. 11 is a graph showing hepatic G6Pase activity in GSD-Ia mice transduced with rAAV. GSD-Ia mice were transduced with a rAAV8 vector (10^{13} vg/kg) expressing either the native or the codon-optimized (co) human G6Pase directed by the GPE promoter/enhancer. Hepatic G6Pase activity in 12-week old mice was 165.4 ± 18.2 nmol/min/mg.

FIG. 12 is a graph showing liver weight in 12-week old wild type (+/+) and rAAV-treated GSD-Ia mice.

FIGS. 13A and 13B are graphs showing glucose tolerance fasting blood glucose profiles, respectively, in 12-week old wild type (○) and rAAV8-GPE-co-G6Pase-treated GSD-Ia (●) mice.

SEQUENCE LISTING

The nucleic and amino acid sequences listed in the accompanying sequence listing are shown using standard letter abbreviations for nucleotide bases, and three letter code for amino acids, as defined in 37 C.F.R. 1.822. Only one strand of each nucleic acid sequence is shown, but the complementary strand is understood as included by any reference to the displayed strand. The Sequence Listing is submitted as an ASCII text file, created on November 12, 2014, 39.6 KB. In the accompanying Sequence Listing:

SEQ ID NO: 1 is the nucleotide sequence of the UF11-GPE-G6PC plasmid, including the following features:

ITR – nucleotides 17-163

G6PC promoter/enhancer – nucleotides 182-3045

Stuffer – nucleotides 3051-3184

Date Reçue/Date Received 2021-04-06

Intron – nucleotides 3185-3321

Stuffer – nucleotides 3322-3367

G6PC coding sequence – nucleotides 3368-4441

ITR – nucleotides 4674-4819

SEQ ID NO: 2 is the nucleotide sequence of the UF11-K29-G6PC plasmid, including the following features:

ITR – nucleotides 17-163

G6PC promoter/enhancer – nucleotides 182-3045

Intron – nucleotides 3052-3188

G6PC coding sequence – nucleotides 3202-4275

ITR – nucleotides 4508-4653

SEQ ID NO: 3 is the nucleotide sequence of the UF11-GPE-co-G6PC plasmid, including the following features:

ITR – nucleotides 17-163

G6PC promoter/enhancer – nucleotides 182-3045

Stuffer – nucleotides 3051-3184

Intron – nucleotides 3185-3321

Stuffer – nucleotides 3322-3367

G6PC coding sequence – nucleotides 3368-4441

ITR – nucleotides 4674-4819

SEQ ID NO: 4 is the amino acid sequence of the human G6PC protein.

SEQ ID NOs: 5-8 are primer sequences.

SEQ ID NO: 9 is the nucleotide sequence of canine G6PC.

SEQ ID NO: 10 is the amino acid sequence of canine G6PC.

DETAILED DESCRIPTION

I. Abbreviations

AAV	adeno-associated virus
BMI	body mass index
CBA	chicken β-actin
CMV	cytomegalovirus
ELISA	enzyme linked immunosorbent assay
G6P	glucose-6-phosphate
G6PC	glucose-6-phosphatase, catalytic subunit

G6PT	glucose-6-phosphate transporter
GPE	G6PC promoter/enhancer
GSD	glycogen storage disease
H&E	hematoxylin & eosin
HCA	hepatocellular adenoma
HCC	hepatocellular carcinoma
ITR	inverted terminal repeat
ORF	open reading frame
rAAV	recombinant AAV
vg	viral genomes
vp	viral particles

II. Terms and Methods

Unless otherwise noted, technical terms are used according to conventional usage. Definitions of common terms in molecular biology may be found in Benjamin Lewin, *Genes V*, published by Oxford University Press, 1994 (ISBN 0-19-854287-9); Kendrew *et al.* (eds.), *The Encyclopedia of Molecular Biology*, published by Blackwell Science Ltd., 1994 (ISBN 0-632-02182-9); and Robert A. Meyers (ed.), *Molecular Biology and Biotechnology: a Comprehensive Desk Reference*, published by VCH Publishers, Inc., 1995 (ISBN 1-56081-569-8).

In order to facilitate review of the various embodiments of the disclosure, the following explanations of specific terms are provided:

Adeno-associated virus (AAV): A small, replication-defective, non-enveloped virus that infects humans and some other primate species. AAV is not known to cause disease and elicits a very mild immune response. Gene therapy vectors that utilize AAV can infect both dividing and quiescent cells and can persist in an extrachromosomal state without integrating into the genome of the host cell. These features make AAV an attractive viral vector for gene therapy. There are currently 11 recognized serotypes of AAV (AAV1-11).

Administration/Administer: To provide or give a subject an agent, such as a therapeutic agent (*e.g.* a recombinant AAV), by any effective route. Exemplary routes of administration include, but are not limited to, injection (such as subcutaneous, intramuscular, intradermal, intraperitoneal, and intravenous), oral, intraductal, sublingual, rectal, transdermal, intranasal, vaginal and inhalation routes.

Codon-optimized: A "codon-optimized" nucleic acid refers to a nucleic acid sequence that has been altered such that the codons are optimal for expression in a particular system (such

as a particular species or group of species). For example, a nucleic acid sequence can be optimized for expression in mammalian cells or in a particular mammalian species (such as human cells). Codon optimization does not alter the amino acid sequence of the encoded protein.

Enhancer: A nucleic acid sequence that increases the rate of transcription by increasing the activity of a promoter.

G6PC: A gene located on human chromosome 17q21 that encodes glucose-6-phosphatase-α (G6Pase-α). G6Pase-α is a 357 amino acid hydrophobic protein having 9 helices that anchor it in the endoplasmic reticulum (Chou *et al.*, *Nat Rev Endocrinol* 6:676-688, 2010). The G6Pase-α protein catalyzes the hydrolysis of glucose 6-phosphate to glucose and phosphate in the terminal step of gluconeogenesis and glycogenolysis and is a key enzyme in glucose homeostasis. Mutations in the G6PC gene cause glycogen storage disease type Ia (GSD-Ia), which is a metabolic disorder characterized by severe fasting hypoglycemia associated with the accumulation of glycogen and fat in the liver and kidneys.

Glycogen storage disease (GSD): A group of diseases that result from defects in the processing of glycogen synthesis or breakdown within muscles, liver and other tissues. GSD can either be genetic or acquired. Genetic GSD is caused by any inborn error of metabolism involved in these processes. There are currently 11 recognized glycogen storage diseases (GSD type I, II, III, IV, V, VI, VII, IX, XI, XII and XIII). GSD-I consists of two autosomal recessive disorders, GSD-Ia and GSD-Ib (Chou *et al.*, *Nat Rev Endocrinol* 6:676-688, 2010). GSD-Ia results from a deficiency in glucose-6-phosphatase-α. Deficiencies in the glucose-6-phosphate transporter (G6PT) are responsible for GSD-Ib.

Glycogen storage disease type Ia (GSD-Ia): Also known as von Gierke disease, GSD-Ia is the most common glycogen storage disease, having an incidence of about 1 in 100,000 live births. GSD-Ia is a genetic disease resulting from deficiency of the enzyme glucose-6-phosphatase-α (G6Pase-α). Deficiency in G6Pase-α impairs the ability of the liver to produce free glucose from glycogen and from gluconeogenesis. Patients affected by GSD-Ia are unable to maintain glucose homeostasis and present with fasting hypoglycemia, growth retardation, hepatomegaly, nephromegaly, hyperlipidemia, hyperuricemia, and lactic academia (Chou *et al.*, *Nat Rev Endocrinol* 6:676-688, 2010). There is currently no cure for GSD-Ia.

Intron: A stretch of DNA within a gene that does not contain coding information for a protein. Introns are removed before translation of a messenger RNA.

Inverted terminal repeat (ITR): Symmetrical nucleic acid sequences in the genome of adeno-associated viruses required for efficient replication. ITR sequences are located at each

end of the AAV DNA genome. The ITRs serve as the origins of replication for viral DNA synthesis and are essential *cis* components for generating AAV integrating vectors.

Isolated: An "isolated" biological component (such as a nucleic acid molecule, protein, virus or cell) has been substantially separated or purified away from other biological components in the cell or tissue of the organism, or the organism itself, in which the component naturally occurs, such as other chromosomal and extra-chromosomal DNA and RNA, proteins and cells. Nucleic acid molecules and proteins that have been "isolated" include those purified by standard purification methods. The term also embraces nucleic acid molecules and proteins prepared by recombinant expression in a host cell as well as chemically synthesized nucleic acid molecules and proteins.

Operably linked: A first nucleic acid sequence is operably linked with a second nucleic acid sequence when the first nucleic acid sequence is placed in a functional relationship with the second nucleic acid sequence. For instance, a promoter is operably linked to a coding sequence if the promoter affects the transcription or expression of the coding sequence. Generally, operably linked DNA sequences are contiguous and, where necessary to join two protein-coding regions, in the same reading frame.

Pharmaceutically acceptable carrier: The pharmaceutically acceptable carriers (vehicles) useful in this disclosure are conventional. *Remington's Pharmaceutical Sciences*, by E. W. Martin, Mack Publishing Co., Easton, PA, 15th Edition (1975), describes compositions and formulations suitable for pharmaceutical delivery of one or more therapeutic compounds, molecules or agents.

In general, the nature of the carrier will depend on the particular mode of administration being employed. For instance, parenteral formulations usually comprise injectable fluids that include pharmaceutically and physiologically acceptable fluids such as water, physiological saline, balanced salt solutions, aqueous dextrose, glycerol or the like as a vehicle. For solid compositions (for example, powder, pill, tablet, or capsule forms), conventional non-toxic solid carriers can include, for example, pharmaceutical grades of mannitol, lactose, starch, or magnesium stearate. In addition to biologically-neutral carriers, pharmaceutical compositions to be administered can contain minor amounts of non-toxic auxiliary substances, such as wetting or emulsifying agents, preservatives, and pH buffering agents and the like, for example sodium acetate or sorbitan monolaurate.

Preventing, treating or ameliorating a disease: "Preventing" a disease (such as GSD-Ia) refers to inhibiting the full development of a disease. "Treating" refers to a therapeutic intervention that ameliorates a sign or symptom of a disease or pathological condition after it has

begun to develop. "Ameliorating" refers to the reduction in the number or severity of signs or symptoms of a disease.

Promoter: A region of DNA that directs/initiates transcription of a nucleic acid (*e.g.* a gene). A promoter includes necessary nucleic acid sequences near the start site of transcription. Typically, promoters are located near the genes they transcribe. A promoter also optionally includes distal enhancer or repressor elements which can be located as much as several thousand base pairs from the start site of transcription.

Purified: The term "purified" does not require absolute purity; rather, it is intended as a relative term. Thus, for example, a purified peptide, protein, virus, or other active compound is one that is isolated in whole or in part from naturally associated proteins and other contaminants. In certain embodiments, the term "substantially purified" refers to a peptide, protein, virus or other active compound that has been isolated from a cell, cell culture medium, or other crude preparation and subjected to fractionation to remove various components of the initial preparation, such as proteins, cellular debris, and other components.

Recombinant: A recombinant nucleic acid molecule is one that has a sequence that is not naturally occurring or has a sequence that is made by an artificial combination of two otherwise separated segments of sequence. This artificial combination can be accomplished by chemical synthesis or by the artificial manipulation of isolated segments of nucleic acid molecules, such as by genetic engineering techniques.

Similarly, a recombinant virus is a virus comprising sequence (such as genomic sequence) that is non-naturally occurring or made by artificial combination of at least two sequences of different origin. The term "recombinant" also includes nucleic acids, proteins and viruses that have been altered solely by addition, substitution, or deletion of a portion of a natural nucleic acid molecule, protein or virus. As used herein, "**recombinant AAV**" refers to an AAV particle in which a recombinant nucleic acid molecule (such as a recombinant nucleic acid molecule encoding G6Pase-α) has been packaged.

Sequence identity: The identity or similarity between two or more nucleic acid sequences, or two or more amino acid sequences, is expressed in terms of the identity or similarity between the sequences. Sequence identity can be measured in terms of percentage identity; the higher the percentage, the more identical the sequences are. Sequence similarity can be measured in terms of percentage similarity (which takes into account conservative amino acid substitutions); the higher the percentage, the more similar the sequences are. Homologs or orthologs of nucleic acid or amino acid sequences possess a relatively high degree of sequence identity/similarity when aligned using standard methods. This homology is more significant when the orthologous proteins

or cDNAs are derived from species which are more closely related (such as human and mouse sequences), compared to species more distantly related (such as human and *C. elegans* sequences).

Methods of alignment of sequences for comparison are well known in the art. Various programs and alignment algorithms are described in: Smith & Waterman, *Adv. Appl. Math.* 2:482, 1981; Needleman & Wunsch, *J. Mol. Biol.* 48:443, 1970; Pearson & Lipman, *Proc. Natl. Acad. Sci. USA* 85:2444, 1988; Higgins & Sharp, *Gene*, 73:237-44, 1988; Higgins & Sharp, *CABIOS* 5:151-3, 1989; Corpet *et al.*, *Nuc. Acids Res.* 16:10881-90, 1988; Huang *et al. Computer Appls. in the Biosciences* 8, 155-65, 1992; and Pearson *et al.*, *Meth. Mol. Bio.* 24:307-31, 1994. Altschul *et al.*, *J. Mol. Biol.* 215:403-10, 1990, presents a detailed consideration of sequence alignment methods and homology calculations.

The NCBI Basic Local Alignment Search Tool (BLAST) (Altschul *et al.*, *J. Mol. Biol.* 215:403-10, 1990) is available from several sources, including the National Center for Biological Information (NCBI) and on the internet, for use in connection with the sequence analysis programs blastp, blastn, blastx, tblastn and tblastx. Additional information can be found at the NCBI web site.

Serotype: A group of closely related microorganisms (such as viruses) distinguished by a characteristic set of antigens.

Stuffer sequence: Refers to a sequence of nucleotides contained within a larger nucleic acid molecule (such as a vector) that is typically used to create desired spacing between two nucleic acid features (such as between a promoter and a coding sequence), or to extend a nucleic acid molecule so that it is of a desired length. Stuffer sequences do not contain protein coding information and can be of unknown/synthetic origin and/or unrelated to other nucleic acid sequences within a larger nucleic acid molecule.

Subject: Living multi-cellular vertebrate organisms, a category that includes human and non-human mammals.

Synthetic: Produced by artificial means in a laboratory, for example a synthetic nucleic acid can be chemically synthesized in a laboratory.

Therapeutically effective amount: A quantity of a specified pharmaceutical or therapeutic agent (*e.g.* a recombinant AAV) sufficient to achieve a desired effect in a subject, or in a cell, being treated with the agent. The effective amount of the agent will be dependent on several factors, including, but not limited to the subject or cells being treated, and the manner of administration of the therapeutic composition.

Vector: A vector is a nucleic acid molecule allowing insertion of foreign nucleic acid without disrupting the ability of the vector to replicate and/or integrate in a host cell. A vector

can include nucleic acid sequences that permit it to replicate in a host cell, such as an origin of replication. A vector can also include one or more selectable marker genes and other genetic elements. An expression vector is a vector that contains the necessary regulatory sequences to allow transcription and translation of inserted gene or genes. In some embodiments herein, the vector is an AAV vector.

Unless otherwise explained, all technical and scientific terms used herein have the same meaning as commonly understood by one of ordinary skill in the art to which this disclosure belongs. The singular terms "a," "an," and "the" include plural referents unless context clearly indicates otherwise. "Comprising A or B" means including A, or B, or A and B. It is further to be understood that all base sizes or amino acid sizes, and all molecular weight or molecular mass values, given for nucleic acids or polypeptides are approximate, and are provided for description. Although methods and materials similar or equivalent to those described herein can be used in the practice or testing of the present disclosure, suitable methods and materials are described below In case of conflict, the present specification, including explanations of terms, will control. In addition, the materials, methods, and examples are illustrative only and not intended to be limiting.

III. Overview of Several Embodiments

Provided herein are recombinant nucleic acid molecules, AAV vectors and recombinant AAV that can be used in gene therapy applications for the treatment of glycogen storage disease, specifically GSD-Ia.

The recombinant nucleic acid molecules include a G6PC promoter/enhancer (GPE), a synthetic intron, and the G6PC coding region. The G6PC coding region is optionally codon-optimized for expression in human cells. The recombinant nucleic acid molecules further include stuffer nucleic acid sequence situated between the G6PC promoter/enhancer and the intron, as well as between the intron and the G6PC coding sequence. The recombinant nucleic acid molecules can further include 5' and 3' inverted terminal repeat (ITR) sequences when encompassed within an AAV vector.

It is disclosed herein that a G6Pase-α expressing recombinant AAV with the G6PC promoter/enhancer (AAV-GPE) is significantly more efficient in directing *in vivo* hepatic transgene expression than another G6Pase-α expressing recombinant AAV having an alternative promoter/enhancer (*i.e.* the chicken β-actin promoter/CMV enhancer). Over a 24-week study

Date Reçue/Date Received 2021-04-06

period, G6PC-deficient mice (a model for GSD-Ia) treated with AAV-GPE exhibited complete normalization of hepatic G6PC deficiency as evidenced by normal levels of blood glucose, blood metabolites, hepatic glycogen and hepatic fat (see Example 1 and Yiu *et al.*, *Mol Ther* 18:1076-1084, 2010). Furthermore, a longer-term study of AAV-GPE-treated $G6pc^{-/-}$ mice demonstrated that gene therapy mediated by AAV-GPE was efficacious for at least 70-90 weeks in mice expressing more than 3% hepatic G6Pase-α. In particular, AAV-GPE-treated mice exhibited normal hepatic fat storage, normal blood metabolite and glucose tolerance profiles, reduced fasting blood insulin levels, and had no evidence of hepatic abnormalities, such as hepatocellular adenoma (see Example 2 and Lee *et al.*, *Hepatology* 56:1719-1729, 2012).

Further disclosed herein is the finding that the upstream enhancer elements of the G6PC promoter are critical for optimal G6PC expression in an animal model of GSD-Ia. Specifically, it is demonstrated that treatment with AAV-GPE, which comprises the G6PC promoter/enhancer at nucleotides -2684 to -1 (relative to the G6PC start site) produces significantly higher levels of hepatic G6Pase-α expression, achieved greater reduction in hepatic glycogen accumulation, and led to a better toleration of fasting in a mouse model of GSD-Ia, compared to a G6Pase-α expressing recombinant AAV containing only a 383 bp minimal G6PC promoter/enhancer (see Example 3 and Lee *et al.*, *Mol Genet Metab.* 110(3):275-280, 2013).

Also disclosed herein is the finding that stuffer nucleotide sequences present between the G6PC promoter/enhancer and the intron, as well as between the intron and the G6PC coding sequence, are important for liver transduction and expression of G6Pase-α. In particular, recombinant AAV produced from plasmid UF11-K29-G6PC (SEQ ID NO: 2) which lacks the stuffer sequences, exhibited G6Pase activity of 7.3 nmol/min/mg. In comparison, recombinant AAV produced from plasmid UF11-GPE-G6PC (SEQ ID NO: 1) exhibited G6Pase activity of 33.0 nmol/min/mg (see Example 4). The present disclosure provides the first description of the stuffer sequences present in the AAV vectors set forth herein as SEQ ID NO: 1 and SEQ ID NO: 3.

In addition, data disclosed herein demonstrates that codon-optimization of the G6PC coding sequence increases efficiency of translation approximately 1.5- to 2.5-fold, resulting in significantly greater G6Pase-α expression in the liver following administration of AAV-co-GPE (containing a codon-optimized G6PC nucleic acid sequence), compared with administration of AAV-GPE, which encodes wild-type G6PC (see Example 5).

Taken together, these results indicate that recombinant AAV comprising the G6PC promoter/enhancer at nucleotides -2684 to -1, a synthetic intron, stuffer sequences flanking the

intron, and the G6PC coding region (wild-type or codon-optimized) are critical features for efficient hepatic transgene expression and treatment of GSD-Ia *in vivo*.

Provided herein are recombinant nucleic acid molecules comprising a nucleotide sequence that is at least 80%, at least 85%, at least 90%, at least 95%, at least 96%, at least 97%, at least 98% or at least 99% identical to nucleotides 182-4441 of SEQ ID NO: 1 or nucleotides 182-4441 of SEQ ID NO: 3. For example, the nucleic acid molecule may contain nucleotide substitutions within the G6PC coding region, such as for codon optimization. As another example, the G6PC coding region may be a G6PC from a different species, such as canine G6PC or a codon-optimized (for expression in humans) version of canine G6PC. In some examples, the G6PC coding region set forth as nucleotides 182-3045 SEQ ID NO: 1 or nucleotides 182-3045 of SEQ ID NO: 3 is replaced with the canine G6PC coding sequence (SEQ ID NO: 9). Alternatively, the human G6PC coding region of SEQ ID NO: 1 or SEQ ID NO: 3 can contain nucleotide substitutions that result in coding changes at residues that differ between the canine and human G6PC protein sequences. For example, nucleotide substitutions can be introduced to result in coding changes at residues 3, 54, 139, 196, 199, 242, 247, 292, 298, 301, 318, 324, 332, 347, 349, 350 and/or 353 of the human G6PC protein (SEQ ID NO: 4). FIG. 9 shows an alignment of the human and canine G6Pase-α protein sequences and FIG. 10 provides a table showing the amino acid differences between human, mouse, rat and canine G6Pase-α. The present disclosure contemplates nucleotide substitutions that alter the amino acid sequence at any of the residues listed in FIG. 10.

In other instances, nucleotide substitutions may be present in the stuffer sequence or in the sequence of the synthetic intron. Nucleotide substitutions are also likely to be tolerated within the vector sequence, such as vector sequence downstream (*i.e.* 3' to) the 3' ITR, or between the 5' ITR and GPE, or between the G6PC coding region and the 3' ITR. In some embodiments, the recombinant nucleic acid molecules comprise nucleotides 182-4441 of SEQ ID NO: 1 or nucleotides 182-4441 of SEQ ID NO: 3. These recombinant nucleic acid molecules include the sequence of the G6PC promoter/enhancer at nucleotides -2684 to -1, a synthetic intron, stuffer sequences flanking the intron, and the G6PC coding region. SEQ ID NO: 1 includes a wild-type G6PC coding sequence, while SEQ ID NO: 3 includes a codon-optimized G6PC coding sequence.

In some embodiments, the recombinant nucleic acid molecules further include 3' and 5' ITR sequences. Thus, provided are recombinant nucleic acid molecules comprising a nucleotide sequence that is at least 80%, at least 85%, at least 90%, at least 95%, at least 96%, at least 97%, at least 98% or at least 99% identical to nucleotides 17-4819 of SEQ ID NO: 1 or nucleotides

17-4819 of SEQ ID NO: 3. In some embodiments, the recombinant nucleic acid molecules comprise nucleotides 17-4819 of SEQ ID NO: 1 or nucleotides 17-4819 of SEQ ID NO: 3. In particular non-limiting examples, the recombinant nucleic acid molecules comprise the complete sequence of SEQ ID NO: 1 (the UF11-GPE-G6PC plasmid used to generate AAV-GPE) or SEQ ID NO: 3 (the UF11-GPE-co-G6PC plasmid used to generate codon-optimized AAV-co-GPE). In other examples, the recombinant nucleic acid molecules comprise a nucleotide sequence that is at least 80%, at least 85%, at least 90%, at least 95%, at least 96%, at least 97%, at least 98% or at least 99% identical to SEQ ID NO: 1 or SEQ ID NO: 3.

In other embodiments, provided is a recombinant nucleic acid molecule comprising a nucleotide sequence that is at least 80%, at least 85%, at least 90%, at least 95%, at least 96%, at least 97%, at least 98% or at least 99% identical to nucleotides 182-4275 of SEQ ID NO: 2. In some examples, the recombinant nucleic molecule comprises nucleotides 182-4275 of SEQ ID NO: 2. In some examples, the recombinant nucleic acid molecule comprises a nucleotide sequence that is at least 80%, at least 85%, at least 90%, at least 95%, at least 96%, at least 97%, at least 98% or at least 99% identical to nucleotides 17-4653 of SEQ ID NO: 2. In some examples, the recombinant nucleic acid molecule comprises nucleotides 17-4653 of SEQ ID NO: 2. In specific non-limiting examples, the recombinant nucleic acid molecule comprises the complete sequence of SEQ ID NO: 2 (the UF11-K29-G6PC plasmid that lacks stuffer sequence). In other examples, the recombinant nucleic acid molecule comprises a nucleotide sequence that is at least 80%, at least 85%, at least 90%, at least 95%, at least 96%, at least 97%, at least 98% or at least 99% identical to SEQ ID NO: 2.

Further provided are vectors comprising the recombinant nucleic acid molecules disclosed herein. In some embodiments, the vector is an AAV vector. The AAV serotype can be any suitable serotype for delivery of transgenes to a subject. In some examples, the AAV vector is a serotype 8 AAV (AAV8). In other examples the AAV vector is a serotype 1, 2, 3, 4, 5, 6, 7, 9, 10, 11 or 12 vector (*i.e.* AAV1, AAV2, AAV3, AAV4, AAV5, AAV6, AAV7, AAV9, AAV10, AAV11 or AAV12). In yet other examples, the AAV vector is a hybrid of two or more AAV serotypes (such as, but not limited to AAV2/1, AAV2/7, AAV2/8 or AAV2/9). The selection of AAV serotype will depend in part on the cell type(s) that are targeted for gene therapy. For treatment of GSD-Ia, the liver and kidney are the relevant target organs.

Also provided herein are isolated host cells comprising the recombinant nucleic acid molecules or vectors disclosed herein. For example, the isolated host cell can be a cell (or cell line) appropriate for production of recombinant AAV (rAAV). In some examples, the host cell

is a mammalian cell, such as a HEK-293, BHK, Vero, RD, HT-1080, A549, Cos-7, ARPE-19, or MRC-5 cell.

Further provided are rAAV comprising a recombinant nucleic acid molecule disclosed herein. In some embodiments, the rAAV is rAAV8 and/or rAAV2. However, the AAV serotype can be any other suitable AAV serotype, such as AAV1, AAV2, AAV3, AAV4, AAV5, AAV6, AAV7, AAV9, AAV10, AAV11 or AAV12, or a hybrid of two or more AAV serotypes (such as, but not limited to AAV2/1, AAV2/7, AAV2/8 or AAV2/9). Compositions comprising a rAAV disclosed herein and a pharmaceutically acceptable carrier are also provided by the present disclosure. In some embodiments, the compositions are formulated for intravenous or intramuscular administration. Suitable pharmaceutical formulations for administration of rAAV can be found, for example, in U.S. Patent Application Publication No. 2012/0219528.

Further provided are methods of treating a subject diagnosed with a glycogen storage disease, comprising selecting a subject with GSD-Ia and administering to the subject a therapeutically effective amount of a rAAV (or a composition comprising a rAAV) disclosed herein. In some embodiments, the rAAV is administered intravenously.

In some embodiments, the rAAV is administered at a dose of about 1 x 10^{11} to about 1 x 10^{14} viral particles (vp)/kg. In some examples, the rAAV is administered at a dose of about 1 x 10^{12} to about 8 x 10^{13} vp/kg. In other examples, the rAAV is administered at a dose of about 1 x 10^{13} to about 6 x 10^{13} vp/kg. In specific non-limiting examples, the rAAV is administered at a dose of at least about 1 x 10^{11}, at least about 5 x 10^{11}, at least about 1 x 10^{12}, at least about 5 x 10^{12}, at least about 1 x 10^{13}, at least about 5 x 10^{13}, or at least about 1 x 10^{14} vp/kg. In other non-limiting examples, the rAAV is administered at a dose of no more than about 5 x 10^{11}, no more than about 1 x 10^{12}, no more than about 5 x 10^{12}, no more than about 1 x 10^{13}, no more than about 5 x 10^{13}, or no more than about 1 x 10^{14} vp/kg. In one non-limiting example, the rAAV is administered at a dose of about 1 x 1012 vp/kg. The rAAV can be administered in a single dose, or in multiple doses (such as 2, 3, 4, 5, 6, 7, 8, 9 or 10 doses) as needed for the desired therapeutic results.

IV. Recombinant AAV for Gene Therapy Applications

AAV belongs to the family *Parvoviridae* and the genus *Dependovirus*. AAV is a small, non-enveloped virus that packages a linear, single-stranded DNA genome. Both sense and antisense strands of AAV DNA are packaged into AAV capsids with equal frequency.

The AAV genome is characterized by two inverted terminal repeats (ITRs) that flank two open reading frames (ORFs). In the AAV2 genome, for example, the first 125 nucleotides of the ITR are a palindrome, which folds upon itself to maximize base pairing and forms a T-shaped hairpin structure. The other 20 bases of the ITR, called the D sequence, remain unpaired. The ITRs are *cis*-acting sequences important for AAV DNA replication; the ITR is the origin of replication and serves as a primer for second-strand synthesis by DNA polymerase. The double-stranded DNA formed during this synthesis, which is called replicating-form monomer, is used for a second round of self-priming replication and forms a replicating-form dimer. These double-stranded intermediates are processed via a strand displacement mechanism, resulting in single-stranded DNA used for packaging and double-stranded DNA used for transcription. Located within the ITR are the Rep binding elements and a terminal resolution site (TRS). These features are used by the viral regulatory protein Rep during AAV replication to process the double-stranded intermediates. In addition to their role in AAV replication, the ITR is also essential for AAV genome packaging, transcription, negative regulation under non-permissive conditions, and site-specific integration (Daya and Berns, *Clin Microbiol Rev* 21(4):583-593, 2008).

The left ORF of AAV contains the Rep gene, which encodes four proteins – Rep78, Rep 68, Rep52 and Rep40. The right ORF contains the Cap gene, which produces three viral capsid proteins (VP1, VP2 and VP3). The AAV capsid contains 60 viral capsid proteins arranged into an icosahedral symmetry. VP1, VP2 and VP3 are present in a 1:1:10 molar ratio (Daya and Berns, *Clin Microbiol Rev* 21(4):583-593, 2008).

AAV is currently one of the most frequently used viruses for gene therapy. Although AAV infects humans and some other primate species, it is not known to cause disease and elicits a very mild immune response. Gene therapy vectors that utilize AAV can infect both dividing and quiescent cells and persist in an extrachromosomal state without integrating into the genome of the host cell. Because of the advantageous features of AAV, the present disclosure contemplates the use of AAV for the recombinant nucleic acid molecules and methods disclosed herein.

AAV possesses several desirable features for a gene therapy vector, including the ability to bind and enter target cells, enter the nucleus, the ability to be expressed in the nucleus for a prolonged period of time, and low toxicity. However, the small size of the AAV genome limits the size of heterologous DNA that can be incorporated. To minimize this problem, AAV vectors have been constructed that do not encode Rep and the integration efficiency element (IEE). The

ITRs are retained as they are *cis* signals required for packaging (Daya and Berns, *Clin Microbiol Rev* 21(4):583-593, 2008).

Methods for producing rAAV suitable for gene therapy are well known in the art (see, for example, U.S. Patent Application Nos. 2012/0100606; 2012/0135515; 2011/0229971; and 2013/0072548; and Ghosh *et al.*, *Gene Ther* 13(4):321-329, 2006), and can be utilized with the recombinant nucleic acid molecules and methods disclosed herein.

The following examples are provided to illustrate certain particular features and/or embodiments. These examples should not be construed to limit the disclosure to the particular features or embodiments described.

EXAMPLES

Example 1: Complete Normalization of Hepatic G6PC Deficiency of Glycogen Storage Disease Type Ia using Gene Therapy

This example describes a comparison of two AAV vectors expressing G6Pase-α, driven by two different promoters, in efficiency of hepatic gene delivery and expression of G6Pase-α in G6PC-deficient mice. The results demonstrate that the AAV vector with the G6PC promoter/enhancer (AAV-GPE) was more efficient in directing persistent *in vivo* hepatic transgene expression than the AAV vector with the chicken β-actin promoter/CMV enhancer (AAV-CBA). In addition, G6PC-deficient mice treated with AAV-GPE exhibited normal levels of blood glucose, blood metabolites, hepatic glycogen and hepatic fat.

MATERIALS AND METHODS

Construction of pUF11-GPE-G6PC and preparation AAV vectors

The UF11-GPE-G6PC plasmid, containing human G6Pase-α under the control of the human *G6PC* promoter/enhancer was constructed by modifying pUF11-mG6Pase-α-CBA (Ghosh *et al.*, *Gene Ther* 13:321-329, 2006) where the murine G6Pase-α is driven by the CBA promoter/CMV enhancer (Xu *et al.*, *Hum Gene Ther* 12:563-573, 2001) as follows: The Tkp-neo fragment from pUF11-mG6Pase-α-CBA was excised by *Xho*I/*Sph*I digestion, the remaining vector gel purified, polished with T4 DNA polymerase, then self-ligated to yield pUF11-mG6Pase-α-CBA-[Tkp-neo]$^{-/-}$. The mG6Pase-α, along with the CBA promoter/CMV enhancer, in pUF11-mG6Pase-α-CBA-[Tkp-neo]$^{-/-}$ was then substituted with the human G6Pase-α cDNA at 5'-SbfI and 3'-NotI sites, yielding pUF11-G6PC. PCR was then used to clone nucleotides -2864 to -1 of the *G6PC* 5'-flanking region containing the human *G6PC* promoter/enhancer. The

PCR template was a bacterial artificial chromosome containing the human *G6PC* gene (Invitrogen Life Technologies, Carlsbad, CA) and the primer pairs were: 1S (5'-CCTTTGAGAATCCACGGTGT-3'; SEQ ID NO: 5) and 2AS (5'-CCTCATTTCCTTGGCACCTC-3'; SEQ ID NO: 6), that contain additional KpnI and XbaI sites at the 5′ and 3′ ends, respectively. The KpnI-XbaI fragment that contains the *G6PC* promoter/enhancer was then ligated into the KpnI-XbaI linearized pUF11-G6PC, to yield pUF11-G6PC-GPE-1. Next, PCR was used to clone the chimeric intron from the pCI vector (Promega, Madison, WI) using primer pair 3S (5'-AGGTAAGTATCAAGGTTACA-3'; SEQ ID NO: 7) and 4AS (5'-ACCTGTGGAGAGAAAGGCAA-3′; SEQ ID NO: 8) that contain additional SpeI and SbfI sites at the 5′ and 3′ ends, respectively. This chimeric intron was then ligated as a SpeI-SbfI fragment into the SpeI-SbfI linearized large fragment of pUF11-G6PC-GPE-I, to yield pUF11-GPE-G6PC (SEQ ID NO: 1). All constructs were verified by DNA sequencing.

AAV-GPE and AAV-CBA were produced using pUF11-GPE-G6PC and pUF11-mG6Pase-α-CBA, respectively, and generated, purified, and tittered as previously described (Ghosh *et al.*, *Gene Ther* 13:321-329, 2006). Vector genome quantitation was performed using real-time PCR with primers and probes directed against the *G6PC* or the CBA promoter.

Infusion of G6pc$^{-/-}$ mice with AAV vectors

A glucose therapy, that consists of intraperitoneal injection of 25-100 μl of 15% glucose every 12 h, was administered to the *G6pc*$^{-/-}$ mice as described previously (Lei *et al.*, *Nat Genet* 13:203-209, 1996). Mice that survived weaning were given unrestricted access to Mouse Chow (Zeigler Bros., Inc., Gardners, PA).

The AAV vector was infused into 2-day-old *G6pc*$^{-/-}$ mice via the temporal vein, and infused into 2- or 4-week-old *G6pc*$^{-/-}$ mice via the retro-orbital sinus. Age-matched *G6pc*$^{+/+}$/*G6pc*$^{+/-}$ as well as 4- to 6-week-old *G6pc*$^{-/-}$ mice were used as controls. For the virus-infused mice, glucose therapy was terminated immediately after infusion.

Glucose tolerance testing of 12- or 14-week-old AAV-GPE-infused *G6pc*$^{-/-}$ mice consisted of fasting for 6 hours prior to blood sampling, followed by the injection of 0.25 ml of 10% dextrose subcutaneously, and repeated blood sampling via the tail vein every 30 minutes for an additional 2 hours.

Phosphohydrolase assays

Microsome isolation and phosphohydrolase assays were determined essentially as described previously (Lei *et al.*, *Nat Genet* 13:203-209, 1996). Reaction mixtures (100 µl) contained 50 mM cacodylate buffer, pH 6.5, 10 mM G6P and appropriate amounts of microsomal preparations were incubated at 37°C for 10 minutes. Disrupted microsomal membranes were prepared by incubating intact membranes in 0.2% deoxycholate for 20 minutes at 0°C. Non-specific phosphatase activity was estimated by pre-incubating disrupted microsomal preparations at pH 5 for 10 minutes at 37°C, to inactivate the acid labile G6Pase-α.

Enzyme histochemical analysis of G6Pase-α was performed by incubating 10 µm thick liver tissue sections for 10 minutes at room temperature in a solution containing 40 mM Tris-maleate pH 6.5, 10 mM G6P, 300 mM sucrose, and 3.6 mM lead nitrate (Teutsch, *Prog Histochem Cytochem* 14:1-92, 1981). The trapped lead phosphate was visualized following conversion to the brown colored lead sulfide (Teutsch, *Prog Histochem Cytochem* 14:1-92, 1981).

Phenotype analyses

Blood samples were collected from the tail vein. Blood glucose, total cholesterol, and uric acid were analyzed using kits obtained from Thermo Electron (Louisville, CO). Triglycerides were measured with a kit from Sigma Diagnostics (St Louis, MO) and lactate measured by a kit from Trinity Biotech (St. Louis, MO).

For hematoxylin and eosin (H&E) and oil red O staining, liver sections were preserved in 10% neutral buffered formalin, and sectioned at 4-10 microns thickness. The stained sections were visualized using the Axioskop2 plus microscope and the AxioVision 4.5 software (Carl Zeiss, Thornwood, NY). For quantitative histochemical measurement of lipid accumulation, the oil red O stain was converted into pixel density units using Adobe Photoshop CS3 (Adobe System Incorporated, San Jose, CA).

To determine the glycogen content of the liver, tissue was homogenized with HCl, boiled for 10 minutes, and neutralized with sodium acetate to a final pH of 4.5 (Teutsch, *Prog Histochem Cytochem* 14:1-92, 1981). The hydrolyzed tissue was then digested with amylo-α-1,4-α-1,6-glucosidase and the released glucose was measured using a kit obtained from Sigma Diagnostics. Glycogen content is reported as nmol glucosyl units per mg of hepatic protein.

Antibody assays

Antibodies against human or murine G6Pase-α were detected by Western-blot analysis. Microsomal proteins from Ad-human G6Pase-α or Ad-mouse G6Pase-α infected COS-1 cells (Ghosh *et al.*, *J Biol Chem* 277: 32837-32842, 2002) were resolved by electrophoresis through a 12% polyacrylamide-SDS gel and trans-blotted onto polyvinylidene fluoride membranes (Millipore, Bedford, MA). The membrane was placed in a Multiscreen Apparatus (Bio-Rad Laboratories, Hercules, CA) containing multiple channels. The membrane strip under each channel was incubated with a rabbit anti-human G6Pase-α serum (Ghosh *et al.*, *J Biol Chem* 277: 32837-32842, 2002) diluted 1:3000, or serum samples from AAV-GPE-infused or AAV-CBA-infused animals diluted 1:200. Serum samples from untreated *G6pc*$^{-/-}$ and *G6pc*$^{+/+}$/*G6pc*$^{+/-}$ littermates diluted 1:200 were used as controls. After overnight incubation, the membrane strips were then incubated with horseradish peroxidase-conjugated goat anti-rabbit IgG or goat anti-mouse IgG (Kirkegarrd & Perry Laboratories, Gaithersburg, MD). The immunocomplex was visualized by the chemiluminescent system using the SuperSignal™ West Pico Chemiluminescent substrate from Pierce (Rockford, IL).

CD8+ lymphocyte immunodetection

Mouse livers were snap frozen, embedded in O.C.T. (Sakura Finetek, Terrance, CA), and sectioned at 8 micron thickness. The sections were fixed in acetone for 10 minutes at -20°C, dried, washed with PBS, blocked with PBS containing 2% of BSA for 30 minutes, and incubated at 4°C overnight with a rabbit polyclonal antibody against CD8 (Abcam Inc., Cambridge, MA) in PBS supplemented with 1% BSA. After washes with PBS, the sections were incubated for 1 hour at 25°C in the dark with a goat anti-rat IgG antibody conjugated with Alexa Fluor® 488 (Invitrogen) dye. Following washes with PBS, the labeled cells were mounted with an anti-fade, water-based mounting medium containing DAPI (Vector Laboratories, Burlingame, CA) and visualized using the Axioskop2 plus fluorescence microscope (Carl Zeiss, Thornwood, NY). The CD8+ cells were counted in ten randomly selected fields at 200-fold magnification and reported as the mean average.

Statistical analysis

The unpaired t test was performed using the GraphPad Prism® Program, version 4 (GraphPad Software, San Diego, CA). Values were considered statistically significant at $p < 0.05$.

RESULTS

AAV-GPE infusion directs long-term hepatic G6Pase-α expression

To examine the *in vivo* impact of sequences upstream of nucleotides -298 of the human *G6PC* promoter element previously studied (Koeberl *et al.*, *Mol Ther* 16:665-672, 2008), AAV-GPE, an AAV8 vector expressing human G6Pase-α under the control of nucleotides -2864 to -1 of the human *G6PC* 5'-flanking region, was constructed. Since there is no standard age at which to initiate AAV-mediated gene therapy in mice (Ghosh *et al.*, *Gene Ther* 13:321-329, 2006; Koeberl *et al.*, *Gene Ther* 13:1281-1289, 2006; Koeberl *et al.*, *Mol Ther* 16:665-672, 2008) and there is evidence that the loss of efficiency and persistence of gene transfer is influenced by the increased rate of hepatocellular proliferation associated with liver growth (Cunningham *et al.*, *Mol Ther* 16:1081-1088, 2008), $G6pc^{-/-}$ mice were infused at three different ages, 2-day-old, 2-week-old, or 4-week-old, and hepatic G6Pase-α expression was examined out to 24 weeks of age. Despite the difference in age, each group of mice was infused with the same dose of AAV-GPE (1.2×10^{11} viral genomes (vg)/mouse). Metabolic profiles of the infused animals were monitored during the 24-week study and all measurements compared to those of their $G6pc^{+/+}$/$G6pc^{+/-}$ littermates and 4 to 6 week-old untreated $G6pc^{-/-}$ mice. GSD-Ia is an autosomal recessive disorder and previous studies have shown that the phenotype of the $G6pc^{+/+}$ and $G6pc^{+/-}$ littermates are indistinguishable and wild type (Lei *et al.*, *Nat Genet* 13:203-209, 1996).

There were no premature deaths in the infused $G6pc^{-/-}$ animals for the duration of the 24-week study, regardless of the age of infusion. In $G6pc^{-/-}$ mice infused at age 2 days with AAV-GPE (1.2×10^{11} vg/mouse, equivalent to 6×10^{13} vg/kg), hepatic G6Pase-α activity was 77.6% of control activity at age 2 weeks, declining to 16.2% at age 4-weeks and 6.5% of control activity at age 6 weeks (Table 1). However, beyond 6 weeks the levels of hepatic G6Pase-α activity stabilized out to 24 weeks (Table 1). Therefore expression dropped 11.9-fold over the entire 24 week study, with most of the drop occurring within the first 6 weeks.

In contrast, in $G6pc^{-/-}$ mice infused at age 2 weeks with AAV-GPE (1.2×10^{11} vg/mouse, equivalent to 1.5×10^{13} vg/kg) hepatic G6Pase-α activity 2 weeks post-infusion (at age 4 weeks) was 2.4-fold higher than the activity in their $G6pc^{+/+}$/$G6pc^{+/-}$ littermates (Table 1), reaching 433.4 ± 11.1 nmol/mg/min. While hepatic G6Pase-α activity did subsequently undergo a 2.6-fold decline between ages 4 to 6 weeks, it resulted in a near normal hepatic G6Pase-α activity (174.0 ± 22.4 nmol/mg/min) being maintained from age 6 weeks on for the duration of the 24-week study (Table 1). Similarly, in $G6pc^{-/-}$ mice infused with AAV-GPE at age 4 weeks with the same dosage (1.2×10^{11} vg/mouse, equivalent to 1×10^{13} vg/kg) hepatic G6Pase-α activity at age 24 weeks was 335.6 ± 40.2 nmol/min/mg, 1.9-fold higher than the activity in the control

littermates (Table 1). These findings are consistent with the previous proposal (Cunningham *et al.*, *Mol Ther* 16:1081-1088, 2008) that the loss of efficiency and persistence of gene transfer is influenced by the increased rate of hepatocellular proliferation associated with liver growth. Injections at later stages of development, when the rate of liver growth is lower, resulted in less gene expression loss.

The distribution of the G6Pase-α transgene expression in the liver was investigated. As expected, there was no stainable G6Pase-α activity in the liver sections of untreated *G6pc*$^{-/-}$ mice. In *G6pc*$^{+/+}$/*G6pc*$^{+/-}$ mice, enzyme histochemical analysis showed G6Pase-α distributed throughout the liver but with significantly higher levels in proximity to blood vessels.

In *G6pc*$^{-/-}$ mice infused at age 2 days with AAV-GPE, hepatic G6Pase-α activity was distributed throughout the liver at age 2 weeks. Unlike wild type mice, the expression was uneven with foci that stained stronger than in the control livers. The stained G6Pase-α activity markedly decreased from age 2 to 4 weeks, consistent with a 4.8-fold decline in phosphohydrolase activity (Table 1). Again, the stained G6Pase activity decreased and stabilized at age 6 weeks and older.

In *G6pc*$^{-/-}$ mice infused with AAV-GPE at age 2 or 4 weeks, enzyme histochemical analyses again showed that the G6Pase-α transgene was distributed throughout the liver with foci containing significantly higher levels of enzymatic activity. Again, G6Pase-α activities estimated by histochemical analyses were in agreement with quantitative phosphohydrolase assays (Table 1). In *G6pc*$^{-/-}$ mice infused with AAV-GPE at age 2 weeks, there were cells in the liver that stained less intensely than cells in the wild type livers. Therefore a normal pattern of hepatic G6Pase-α expression was not restored in AAV-GPE-infused mice despite exhibiting wild type G6Pase-α activity.

Table 1. Hepatic G6Pase activity in *G6pc*$^{-/-}$ mice infused with 1.2 x 10^{11} vg/mouse of AAV-GPE

Mice	Age weeks	Phosphohydrolase Activity nmol/mg/min	Relative Activity %	% (+/+ or +/-) Activity
+/+ or +/- (n = 16)	2-24	178.1 ± 10.0		100
Infusion at age 2 days				
-/-/AAV-GPE (n = 2)	2	138.3 ± 22.6	100	77.6
-/-/AAV-GPE (n = 4)	4	28.8 ± 9.9	20.8	16.2

Mice	Age	Phosphohydrolase Activity	Relative Activity	% (+/+ or +/-) Activity
	weeks	nmol/mg/min	%	
-/-/AAV-GPE (n = 7)	6-24	11.6 ± 5.0	8.4	6.5
Infusion at age 2 weeks				
-/-/AAV-GPE (n = 2)	4	433.4 ± 11.1	100	243.3
-/-/AAV-GPE (n = 2)	6	156.1 ± 7.0	36.0	87.6
-/-/AAV-GPE (n = 3)	24	174.0 ± 22.4	40.1	97.7
Infusion at age 4 weeks				
-/-/AAV-GPE (n = 3)	24	335.6 ± 40.2		188.4

G6pc$^{-/-}$ (-/-) mice were infused with 1.2 x 10^{11} vg/mouse of AAV-GPE at age 2 days, 2 weeks, or 4 weeks as described under MATERIALS and METHODS. Age-matched *G6pc*$^{+/+}$/*G6pc*$^{+/-}$ (+/+ & +/-) mice were used as positive controls and 4- to 6-week-old *G6pc*$^{-/-}$ (-/-) mice were used as negative controls. Values in the table have been corrected for background by subtracting the G6Pase-α activity (1.8 ± 0.2 *nmol/min/mg*) in the liver microsomes of untreated *G6pc*$^{-/-}$ mice from the respective results. Data are presented as mean ± SEM.

AAV-CBA infusion directs lower levels of hepatic G6Pase-α expression

The CBA promoter/CMV enhancer has been widely used to direct high levels of hepatic transgene expression (Xu *et al.*, *Hum Gene Ther* 12:563-573, 2001). However, the CMV enhancer is known to be silenced by extensive CpG and non-CpG methylation (Brooks *et al.*, *J Gene Med* 6:395-404, 2004; Mehta *et al.*, *Gene* 428: 20-24, 2009). Previous *in vivo* experiments using AAV-CBA, an AAV8 vector expressing murine G6Pase-α under the control of the hybrid CBA promoter/CMV enhancer had shown poor expression (Ghosh *et al.*, *Gene Ther* 13:321-329, 2006), possibly related to CMV promoter methylation. To compare the *in vivo* efficacy of hepatic gene transfer between AAV-CBA and AAV-GPE, *G6pc*$^{-/-}$ mice were infused with an increased dose of AAV-CBA at 4.8 x 10^{11} vg/mouse in a similar manner to the AAV-GPE experiments – at ages 2 days and 2 weeks and followed to 24 weeks of age.

For *G6pc*$^{-/-}$ mice infused at 2 days of age, hepatic G6Pase-α activity at age 2 weeks was 2.8 fold higher in AAV-CBA-infused mice compared to AAV-GPE-infused mice (Tables 1 and 2), reflecting the 4-fold higher dosage of AAV-CBA infused. However, hepatic G6Pase-α activity in the neonatally AAV-CBA-infused animals declined rapidly to 20.6 ± 1.1 nmol/mg/min at age 4 weeks (Table 2), an 18.6-fold decline in 2 weeks, compared to a 4.8-fold decline in neonatal

G6pc$^{-/-}$ mice infused with AAV-GPE (Table 1). Since the CBA and GPE are in identical vector background, this finding suggests that the CBA promoter/CMV enhancer is less efficient in directing persistent *in vivo* hepatic transgene expression than the *G6PC* promoter/enhancer.

In *G6pc*$^{-/-}$ mice infused with 4.8 x 10^{11} vg/mouse of AAV-CBA at age 2 weeks, hepatic G6Pase-α activity was 236.9 ± 64.7 at age 4 weeks (Table 2), which was 1.83-fold lower than 4-week-old *G6pc*$^{-/-}$ mice infused at age 2 weeks with 1.2 x 10^{11} vg/mouse of AAV-GPE (Table 1). Moreover, hepatic G6Pase-α activity continued to decline with the CBA vector from 55.7 ± 2.7 nmol/mg/min at age 6 weeks to 38.1 ± 1.7 nmol/mg/min at age 24 weeks (Table 2). This was in contrast to the levels expressed with the GPE vector that stabilized over this time period at near wild type levels (Table 1).

Enzyme histochemical analyses of AAV-CBA-infused animals showed that the activity staining was similar to those of the GPE vector, unevenly distributed with numerous foci that stained stronger than that in the control livers. But consistent with the quantitative phosphohydrolase assays (Table 2), the overall stain intensities were significantly lower with increasing age of the infused mice.

Table 2. Hepatic G6Pase activity in *G6pc*$^{-/-}$ mice infused with 4.8 x 10^{11} vg/mouse of AAV-CBA

Mice	Age weeks	Phosphohydrolase Activity nmol/mg/min	Relative Activity %	% (+/+ or +/-) Activity
+/+ or +/- (n = 16)	2-24	178.1 ± 10.0		
Infusion at age 2 days				
-/-/AAV-CBA (n = 2)	2	382.3 ± 4.2	100	214.7
-/-/AAV-CBA (n = 3)	4	20.6 ± 1.1	5.4	11.6
Infusion at age 2 weeks				
-/-/AAV-CBA (n = 2)	4	236.9 ± 64.7	100	133.0
-/-/AAV-CBA (n = 2)	6	55.7 ± 2.7	23.5	31.3
-/-/AAV-CBA (n = 3)	24	38.1 ± 1.7	16.1	21.4

G6pc$^{-/-}$ (-/-) mice were infused with 4.8 x 10^{11} vg/mouse of AAV-CBA at age 2 days and 2 weeks as described under MATERIALS and METHODS. Age-matched *G6pc*$^{+/+}$/*G6pc*$^{+/-}$ (+/+ & +/-) mice were used as positive controls and 4- to 6-week-old *G6pc*$^{-/-}$ (-/-) mice were used as

negative controls. Values in the table have been corrected for background by subtracting the G6Pase-α activity (1.8 ± 0.2 *nmol/min/mg*) in the liver microsomes of untreated *G6pc*$^{-/-}$ mice from the respective results. Data are presented as mean ± SEM.

AAV-GPE infusion corrects pathological manifestations of GSD-Ia

G6pc$^{-/-}$ mice under glucose therapy are growth retarded and by 2 weeks of age their average body weight is approximately 60% of their *G6pc*$^{+/+}$/*G6pc*$^{+/-}$ littermates (Lei *et al.*, *Nat Genet* 13:203-209, 1996). Neonatal *G6pc*$^{-/-}$ mice infused with AAV-GPE had a markedly improved growth rate and the body weights of the infused animals were comparable to the control mice (FIG. 1A). *G6pc*$^{-/-}$ mice infused at age 2 or 4 weeks with AAV-GPE exhibited a growth curve that paralleled their *G6pc*$^{+/+}$/*G6pc*$^{+/-}$ littermates but at lower values, consistent with the lower starting body weights of *G6pc*$^{-/-}$ mice before commencing gene therapy (FIG. 1A).

Under glucose therapy, the *G6pc*$^{-/-}$ mice continue to manifest hypoglycemia, hypercholesterolemia, hypertriglyceridemia, hyperuricemia, and lactic academia (Lei *et al.*, *Nat Genet* 13:203-209, 1996; Kim *et al.*, *J Hepatol* 48: 479-485, 2008). In contrast, the AAV-GPE-infused *G6pc*$^{-/-}$ mice had normal blood glucose profiles (FIG. 1B) and none of the infused animals suffered from the frequent hypoglycemic seizures typical of the untreated *G6pc*$^{-/-}$ mice (Lei *et al.*, *Nat Genet* 13:203-209, 1996) and human GSD-Ia patients (Chou *et al.*, *Curr Mol Med* 2:121-143, 2002). Blood glucose levels in neonatally infused *G6pc*$^{-/-}$ mice were significantly lower than their control littermates (FIG. 1B), suggesting that hepatic G6Pase-α activity restored to 6.5% of control levels is insufficient to maintain normal blood glucose profile. In contrast, blood glucose levels in *G6pc*$^{-/-}$ mice infused with AAV-GPE at age 2 or 4 weeks were indistinguishable from those in their control littermates (FIG. 1B). AAV-GPE infusion also normalized serum cholesterol, triglyceride, uric acid, and lactic acid levels, although neonatally infused *G6pc*$^{-/-}$ mice had slightly higher levels of blood cholesterol and lactic acid (FIG. 1B).

Hepatomegaly is another clinical presentation in GSD-Ia and is primarily caused by excess glycogen and lipid deposition (Chou *et al.*, *Curr Mol Med* 2:121-143, 2002). No histological abnormality was observed in the liver tissue sections of the unaffected and AAV-GPE-transduced mice at age 24 weeks. Glycogen content in the liver of 24-week-old *G6pc*$^{+/+}$/*G6pc*$^{+/-}$ mice averaged 1.89 ± 0.17 nmol glucosyl units per mg protein In neonatally AAV-GPE-infused animals the glycogen content at 24 weeks of age was significantly higher at 4.65 ± 0.19 nmol glucosyl units per mg protein, indicative of the glycogen storage defect observed in GSD-Ia mice. In contrast, the mice receiving infusions at 2 or 4 weeks of age showed wild type levels of glycogen at 24 weeks of age, namely 1.61 ± 0.39, and 1.65 ± 0.19 nmol glucosyl units per

mg protein, respectively, indicative of the absence of the characteristic histology of GSD-Ia disease at this stage of development.

Oil red O staining showed that the lipid contents in AAV-GPE-infused animals were similar to that in the *G6pc*$^{+/+}$/*G6pc*$^{+/-}$ littermates at age 24 weeks. For quantitative histochemical measurement, lipid imaged with Oil red O stain was converted into pixel density units using Adobe Photoshop. The density units in the liver of AAV-GPE-treated *G6pc*$^{-/-}$ mice were lower than those in the control mice (approximately 150 pixel density units/μm^2 compared with approximately 300 pixel density units/μm^2), although the difference was not statistically significant. Taken together, these results indicate AAV-GPE-infused *G6pc*$^{-/-}$ mice exhibited no histological abnormality and had normal glycogen and fat contents in the liver.

AAV-GPE-infused G6pc$^{-/-}$ mice exhibit normal fasting glucose and glucose tolerance profile

Fasting blood glucose levels were examined in 12- and 14-week-old *G6pc*$^{-/-}$ mice infused with AAV-GPE at age 2 and 4 weeks, respectively. Blood glucose levels in *G6pc*$^{+/+}$/*G6pc*$^{+/-}$ mice were unchanged after 6 hours of fasting. Importantly, blood glucose levels in *G6pc*$^{-/-}$ mice infused with AAV-GPE at either age 2 or 4 weeks were also unchanged after 6 hours of fasting, demonstrating that the infused *G6pc*$^{-/-}$ mice no longer suffer from fasting hypoglycemia, characteristics of GSD-Ia (Chou *et al.*, *Curr Mol Med* 2:121-143, 2002). Similar fasting experiments with the untreated *G6pc*$^{-/-}$ mice resulted in rapid hypoglycemia followed by hypoglycemic seizures after only a short fast.

Studies have shown that over-expression of hepatic G6Pase-α may induce diabetes (Liu *et al.*, *Biochem Biophys Res Commun* 205:680-686, 1994; Antinozzi *et al.*, *Annu Rev Nutr* 19: 511-544, 1999; Clore *et al.*, *Diabetes* 49:969-974, 2000). Since hepatic G6Pase-α activity in 24-week-old *G6pc*$^{-/-}$ mice infused at age 4 weeks with AAV-GPE was nearly 2-fold higher than the activity in their *G6pc*$^{+/+}$/*G6pc*$^{+/-}$ littermates, we conducted a glucose tolerance test in 14-week-old *G6pc*$^{-/-}$ mice infused at age 4 weeks with AAV-GPE. As a control, a glucose tolerance test was also performed in 12-week-old *G6pc*$^{-/-}$ mice infused at age 2 weeks with AAV-GPE. These animals exhibited wild type levels of hepatic G6Pase-α activity. Glucose tolerance profiles in the infused *G6pc*$^{-/-}$ mice were indistinguishable from that of control littermates.

Absence of immune response against human G6Pase-α

To determine whether a humoral response directed against human G6Pase-α is generated in the infused *G6pc*$^{-/-}$ mice, Western blot analysis was performed using sera from mice infused

with AAV-GPE or AAV-CBA. As a positive control, a rabbit anti-human G6Pase-α antiserum that also recognizes murine G6Pase-α was used (Ghosh *et al.*, *J Biol Chem* 277: 32837-32842, 2002). No antibodies directed against G6Pase-α were detected in any of the AAV-GPE-infused or AAV-CBA-infused *G6pc*$^{-/-}$ mice that lived to age 24 weeks. Furthermore, there were no endogenous antibodies directed against G6Pase-α present in the sera of *G6pc*$^{+/+}$/*G6pc*$^{+/-}$ littermates or untreated *G6pc* $^{-/-}$ mice.

AAV-CBA infusion elicits increased hepatic CD8+ lymphocyte infiltration

The absence of detectable antibodies against G6Pase-α in the liver of AAV-CBA-infused *G6pc*$^{-/-}$ mice suggests that a cell-mediated immune response to the G6Pase-α transgene is not the cause for the rapid decline in transgene expression directed by this vector. Another possibility is an inflammatory immune response elicited by the AAV-CBA vector. Therefore, hepatic CD8+ lymphocyte infiltration was examined 2 weeks following infusion of *G6pc*$^{-/-}$ mice with AAV-CBA or AAV-GPE. In 2- and 4-week-old wild type or *G6pc*$^{-/-}$ mice, hepatic CD8+ lymphocyte counts were low. In *G6pc*$^{-/-}$ mice infused with AAV-CBA or AAV-GPE at age 2 days, hepatic CD8+ lymphocyte counts at age 2 weeks were similar for each of the vector types and comparable to the counts in untreated 2-week-old wild type or *G6pc*$^{-/-}$ animals. In *G6pc*$^{-/-}$ mice infused with AAV-GPE at age 2 weeks, hepatic CD8+ lymphocyte counts remained low at age 4 weeks. In contrast, in *G6pc*$^{-/-}$ mice infused with AAV-CBA at age 2 weeks, hepatic CD8+ lymphocyte counts were markedly increased at age 4 weeks. The results suggest that an inflammatory response elicited by AAV-CBA may explain, at least in part, the rapid decline and low efficacy of hepatic G6Pase-α expression directed by the CBA promoter/CMV enhancer.

Example 2: Prevention of Hepatocellular Adenoma and Correction of Metabolic Abnormalities in Glycogen Storage Disease Type IA using Gene Therapy

This example describes studies to evaluate the efficacy of the AAV-GPE vector in a long-term study. Gene therapy mediated by the AAV-GPE vector in G6pc$^{-/-}$ mice was efficacious for at least 70-90 weeks in mice expressing more than 3% of wild-type hepatic G6Pase-α. The results demonstrated that AAV-GPE treated mice exhibit normal hepatic fat storage, normal blood metabolite and glucose tolerance profiles, reduced fasting blood insulin levels, and no evidence of hepatic abnormalities.

MATERIALS AND METHODS

Infusion of G6pc$^{-/-}$ mice with AAV-GPE

The AAV-GPE vector (as described in Example 1 and Yiu *et al.*, *Mol Ther* 18:1076-1084, 2010) was infused into G6pc$^{-/-}$ mice (Lei *et al.*, *Nat Genet* 13: 203-209, 1996) via the retro-orbital sinus. Age-matched G6pc$^{+/+}$/G6pc$^{+/-}$ as well as 6- to 10-week-old G6pc$^{-/-}$ mice were used as controls. For the virus-infused mice, glucose therapy (Lei *et al.*, *Nat Genet* 13: 203-209, 1996) was terminated immediately after infusion.

Glucose tolerance testing of mice consisted of fasting for 6 hours, prior to blood sampling, followed by intraperitoneal injection of a glucose solution at 2 mg/g body weight, and repeated blood sampling via the tail vein for 2 hours.

Phosphohydrolase and microsomal G6P uptake assays

Microsome isolation, phosphohydrolase assays, enzyme histochemical analysis of G6Pase-α, and microsomal G6P uptake assays were performed as described previously (Yiu *et al.*, *Mol Ther* 18:1076-1084, 2010; Lei *et al.*, *Nat Genet* 13: 203-209, 1996).

Phenotype analyses

Mice were first examined for hepatic nodules by ultrasound using the Vevo 2100 system (VisualSonics, Ontario, Canada) and blood samples were collected from the tail vein. Blood glucose, total cholesterol, and uric acid were analyzed using kits obtained from Thermo Electron (Louisville, CO); triglycerides, by a kit from Sigma Diagnostics (St Louis, MO); lactate, by a kit from Trinity Biotech (St. Louis, MO); and insulin, by an ultra-sensitive mouse insulin ELISA kit from Crystal Chem (Downers Grove, IL). Hepatic glycogen contents were measured as described previously (Yiu *et al.*, *Mol Ther* 18:1076-1084, 2010). To determine hepatic triglyceride, glucose, and G6P contents, liver tissues were homogenized in RIPA buffer (50 mM Tris HCl, pH 8.0, 150 mM NaCl, 1% Triton X-100, 0.5% Na-deoxycholate, and 0.1% SDS) (Thermo Scientific, Rockford, IL), and triglycerides were measured using a kit from Sigma Diagnostics, glucose, by a kit from Thermo Electron, and G6P, by a kit from BioVision (Mountain View, CA).

For hematoxylin and eosin (H&E) and oil red O staining (Yiu *et al.*, *Mol Ther* 18:1076-1084, 2010), liver sections were preserved in 10% neutral buffered formalin and sectioned at 4-10 microns thickness. The stained sections were visualized using the Axioskop2 plus microscope and the AxioVision 4.5 software (Carl Zeiss, Thornwood, NY).

Quantitative real-time RT-PCR and antibody analysis

Total RNAs were isolated from liver tissues using the TRIzol™ Reagent (Invitrogen, Carlsbad, CA). The mRNA expression was quantified by real-time RT-PCR in an Applied Biosystems 7300 Real-Time PCR System using Applied Biosystems TaqMan probes (Foster City, CA). Data were analyzed using the Applied Biosystems SDS v1.3 software and normalized to β-actin RNA. Antibodies against human G6Pase-α were detected by Western-blot analysis as described previously (Yiu *et al.*, *Mol Ther* 18:1076-1084, 2010).

Statistical Analysis

The unpaired t test was performed using the GraphPad Prism® Program, version 4 (San Diego, CA). Values were considered statistically significant at $P < 0.05$.

RESULTS

AAV-GPE infusion directs long-term hepatic G6Pase-α expression

Two- or four-week-old G6pc$^{-/-}$ mice (n = 18) were infused with varying doses of AAV-GPE (5×10^{12} to 3×10^{13} viral particles (vp)/kg) predicted to restore and maintain 3% to 100% of wild type hepatic G6Pase-α activity. One 15-week-old (5×10^{12} vp/kg) and one 30-week-old (1×10^{13} vp/kg) G6pc$^{-/-}$ mouse were also infused. The low survival rate of GSD-Ia mice under glucose therapy severely restricted the numbers of adult mice available to study (Lei *et al.*, *Nat Genet* 13: 203-209, 1996). Metabolic and histological profiles of the 20 infused animals were monitored across 70-90 weeks and all measurements compared to those of their G6pc$^{+/+}$ and G6pc$^{+/-}$ littermates. The phenotype of both G6pc$^{+/+}$ and G6pc$^{+/-}$ mice are indistinguishable from wild type (Lei *et al.*, *Nat Genet* 13: 203-209, 1996).

There were no premature deaths of the AAV-GPE-treated G6pc$^{-/-}$ mice. Hepatic G6Pase-α activity and glycogen content, were assessed in mice sacrificed after a 24 hour fast. The mean fasting hepatic G6Pase-α activity of 70- to 90-week-old wild type mice (n = 20) was 185.8 ± 12.7 nmol/mg/min (FIG. 2A). As planned, there was a range of hepatic G6Pase-α activities restored in the treated mice. Of the 20 AAV-GPE-treated G6pc$^{-/-}$ mice sacrificed at age 70 to 90 weeks, 6 mice had low levels (3% to 9% of wild type activity) of hepatic G6Pase-α activity and were designated AAV-L, 9 mice had medium levels (22% to 63% of wild type activity) of hepatic G6Pase-α activity, designated AAV-M, and 5 mice had high levels (81% to 128% of wild type activity) of hepatic G6Pase-α activity, designated AAV-H (FIG. 2A). Real-time RT-PCR analysis showed a linear relationship between hepatic G6Pase-α mRNA expression and G6Pase-α activity (FIG. 2B).

Enzyme histochemical analysis showed that G6Pase-α in wild type mice was distributed throughout the liver with significantly higher levels in proximity to blood vessels. There was no stainable G6Pase-α activity in the liver sections of untreated $G6pc^{-/-}$ mice. In AAV-GPE-treated $G6pc^{-/-}$ mice, G6Pase-α was also distributed throughout the liver but with foci, not related to blood vessels, containing markedly higher levels of enzymatic activity. The uneven distribution of hepatic G6Pase-α in the AAV-GPE-treated $G6pc^{-/-}$ mice suggests that a substantial proportion of hepatocytes harbored low or little G6Pase-α, including AAV-H livers expressing 81-128% of wild type G6Pase-α activity. Uniform hepatic G6Pase-α expression is not required for rescue of the GSD-Ia phenotype.

AAV-GPE infusion corrects metabolic abnormalities in GSD-Ia

GSD-Ia is characterized by hypoglycemia, hypercholesterolemia, hypertriglyceridemia, hyperuricemia, and lactic academia (Chou *et al.*, *Nat Rev Endocrinol* 6:676-688, 2010). Blood glucose levels in AAV-H mice expressing wild type hepatic G6Pase-α activity were indistinguishable from those of the control littermates (FIG. 3A). AAV-M and AAV-L expressing 22-63% and 3-9% normal hepatic G6Pase-α activity, respectively also maintained a euglycemia (~100 mg/dl) state (Yoshizawa *et al.*, *J Clin Invest* 119:2807-2817, 2009) but their blood glucose levels were consistently lower than the control littermates (FIG. 3A). All AAV-GPE-treated $G6pc^{-/-}$ mice exhibited normal serum profiles of cholesterol and triglyceride, while serum levels of uric acid and lactic acid in the treated $G6pc^{-/-}$ mice were lower than those in the control littermates (FIG. 3A).

The average body weights of female and male AAV-GPE-treated mice at age 70-90 weeks were 70% and 62%, respectively of their age- and sex-matched control mice (FIG. 3B). However, the average body lengths of the treated $G6pc^{-/-}$ mice were 90% of the controls (FIG. 3B). Consequently, body mass index (BMI) values (Bahary *et al.*, *Proc Natl Acad Sci USA* 87:8642-8646, 1990) of AAV-GPE-treated $G6pc^{-/-}$ mice were significantly lower than those of the control littermates (FIG. 3B). While BMI values of both mouse groups signify normal growth (Bahary *et al.*, *Proc Natl Acad Sci USA* 87:8642-8646, 1990), the AAV-GPE-treated $G6pc^{-/-}$ mice were considerably leaner. The liver weights in wild type mice were relatively constant (FIG. 3C). In AAV-GPE-infused mice, liver weights were inversely correlated to the hepatic G6Pase-α activity restored (FIG. 3C). When liver weights were expressed as percent of body weight, AAV-GPE-treated $G6pc^{-/-}$ mice had significantly higher values because of their lower body weights. However, when absolute liver weights were compared directly, there was no significant difference between AAV-M, AAV-H, and control littermates (FIG. 3C). AAV-L mice, however, continued exhibiting

hepatomegaly. AAV-GPE delivers little or no transgene to the kidney (Yiu *et al.*, *Mol Ther* 18:1076-1084, 2010). However, the infused mice expressing higher hepatic G6Pase-α activity had lower kidney weights, suggesting good hepatic metabolic control normalized nephromegaly.

Absence of histological abnormalities, steatosis, or HCA in AAV-GPE-infused G6pc$^{-/-}$ Livers

To determine the presence of HCA nodules in AAV-GPE-treated G6pc$^{-/-}$ mice, ultrasound analysis was conducted, followed by extensive examination of the livers and histological analysis of liver biopsy samples, using 5 or more separate sections per liver. Ultrasound and morphological analyses detected no hepatic nodules in wild type (n = 20) and AAV-GPE-transduced G6pc$^{-/-}$ (n = 20) mice that lived to age 70-90 weeks. The AAV-GPE-treated G6pc$^{-/-}$ mice infused at age 2 or 4 weeks (n = 18) exhibited no hepatic histological abnormalities except increased glycogen storage. The 84-week-old mouse infused at age 15 weeks, which expressed 6% of normal hepatic G6Pase-α activity, exhibited elevated glycogen storage and a few necrotic foci in one liver section. While most of the liver tissue sections of the 90-week-old mouse infused at age 30 weeks, which expressed 38% of normal hepatic G6Pase-α activity, exhibited no histological abnormalities, one liver section did have many necrotic foci. As necrotic foci are a characteristic hepatic pathology seen in untreated GSD-Ia mice age 6 weeks or older (Kim *et al.*, *J Hepatol* 48: 479-485, 2008), it is quite likely that the necrotic foci had developed before initiation of gene therapy at age 15 or 30 weeks.

The livers of liver-specific G6pc-null mice were reported to develop HCA with marked steatosis (Mutel *et al.*, *J Hepatol* 54:529-537, 2011). While a few wild type mice had increased hepatic fat storage, there was little or no fat storage in the livers of AAV-GPE-treated G6pc$^{-/-}$ mice. Moreover, hepatic triglyceride contents in AAV-GPE-treated G6pc$^{-/-}$ mice (n = 20) were not statistically different from those in wild type mice. Oil red O staining confirmed that lipid contents in AAV-GPE-treated animals (n = 20) were similar to that in the controls.

It has been well established that cyclooxygenase-2 (COX-2) is a marker that is over-expressed in many pre-malignant and malignant cancers, including HCC (Wu, *Cancer Treat Rev* 32:28-44, 2006). Quantitative RT-PCR analysis showed that similar levels of hepatic COX-2 message were expressed in AAV-GPE-treated G6pc$^{-/-}$ and control littermates.

AAV-GPE-treated G6pc$^{-/-}$ mice exhibit normal fasting glucose and glucose tolerance profiles

The mean blood glucose levels of wild type mice (n = 20) before commencing fasting were 165.0 ± 3.0 mg/dl (zero time) which decreased to 113.3 ± 6.5 mg/dl after 24 hours of

fasting (FIG. 4A). The fasting blood glucose profiles of AAV-L and AAV-M mice paralleled those of the control mice but blood glucose levels were consistently lower (FIG. 4A), while the fasting glucose profile of AAV-H mice was indistinguishable from that of the control mice. In sharp contrast, untreated G6pc$^{-/-}$ mice exhibited marked hypoglycemia within 60 to 75 minutes of fasting (FIG. 4B), a hallmark of GSD-Ia (Chou *et al.*, *Nat Rev Endocrinol* 6:676-688, 2010). In summary, AAV-GPE-treated G6pc$^{-/-}$ mice no longer suffered from the fasting hypoglycemia characteristic of GSD-Ia (Chou *et al.*, *Nat Rev Endocrinol* 6:676-688, 2010).

Blood glucose tolerance profiles in AAV-M and AAV-H mice were indistinguishable from those of wild-type littermates (FIG. 4C). In AAV-L mice, following intraperitoneal glucose injection, blood glucose levels declined at a faster rate than the wild type controls.

Reduced fasting blood insulin levels in AAV-GPE-treated G6pc$^{-/-}$ mice

Insulin signaling regulates hepatic glucose and lipid metabolism (Leavens and Birnbaum, *Crit Rev Biochem Mol Biol* 46:200-215, 2011). After 24 hours of fasting, blood insulin levels in 70-90-week-old wild type (n = 20) and AAV-GPE-treated G6pc$^{-/-}$ mice (n = 20) were 1.84 ± 0.29 and 0.56 ± 0.09 ng/ml, respectively (FIG. 5A). Both were within the normal range (de Luca *et al.*, *J Clin Invest* 115:3484-3493, 2005), although fasting blood insulin levels in the AAV-GPE-treated G6pc$^{-/-}$ mice were more close to the normal average values (de Luca *et al.*, *J Clin Invest* 115:3484-3493, 2005). While fasting blood insulin levels in AAV-GPE-treated G6pc$^{-/-}$ mice did not correlate with hepatic G6Pase-α restored, insulin levels in wild type and the treated G6pc$^{-/-}$ mice exhibited a linear relationship to their body weights (FIG. 5A).

The transcriptional effect of insulin is mediated by sterol regulatory element binding protein-1c (SREBP-1c) (Leavens and Birnbaum, *Crit Rev Biochem Mol Biol* 46:200-215, 2011). Quantitative RT-PCR analysis showed that similar levels of hepatic SREBP-1c transcripts were expressed in the 24-hour-fasted AAV-GPE-treated G6pc$^{-/-}$ and control mice (FIG. 5B). Glucokinase is a glucose sensor (Massa *et al.*, *IUBMB Life* 63:1-6, 2011). Hepatic glucokinase activity decreases when blood insulin levels are low, as when fasting (Massa *et al.*, *IUBMB Life* 63:1-6, 2011). As was seen with blood insulin, after 24 hours of fast, hepatic glucokinase transcripts in AAV-GPE-treated *G6pc*$^{-/-}$ mice were significantly lower than that in the control littermates (FIG. 5C). Interestingly, levels of hepatic glucokinase mRNA and fasting blood insulin exhibited a linear relationship in both wild-type and AAV-GPE-treated G6pc$^{-/-}$ mice (FIG. 5C).

Glucose homeostasis in the liver of AAV-GPE-infused G6pc$^{-/-}$ mice

During fasting, blood glucose homeostasis is maintained by endogenous glucose produced in the liver from hydrolysis of G6P by the G6PT/G6Pase-α complex in the terminal step of gluconeogenesis and glycogenolysis (Chou *et al.*, *Nat Rev Endocrinol* 6:676-688, 2010). G6pc$^{-/-}$ mice, lacking a functional G6Pase-α, are incapable of producing endogenous glucose in the liver, kidney, or intestine. After 24 hours of fast, hepatic free glucose levels in wild type mice (n = 20) were 389 ± 17 nmol/mg protein and in AAV-L (n = 6), AAV-M (n = 9), and AAV-H (n = 5) mice were 61%, 68% and 90%, respectively, of that in wild type mice. Intracellular G6P levels in the fasted AAV-L and AAV-M livers were 2.9- and 1.6-fold, respectively higher than wild type livers but intracellular G6P levels in the fasted AAV-H livers were statistically similar to that of wild type livers.

Hepatic G6P participates in several metabolic pathways, including glycogen synthesis, glycolysis, the pentose-phosphate pathway, in the cytoplasm and endogenous glucose production in the ER lumen. Hepatic expression of several key enzymes involved in the above mentioned pathways was examined in mice after a 24-hour fast. These included the cytosolic phosphoenolpyruvate carboxykinase (PEPCK-C) that catalyzes the first committed step in hepatic gluconeogenesis (Hanson and Reshef, *Biochimie* 85:1199-1205, 2003); fructose-1,6-bisphosphatase (FBPase-1) that converts fructose-1,6-bisphosphate to fructose-6-phosphate (Hers, J *Inherit Metab Dis* 13:395-410, 1990); phosphoglucomutase (PGMase) that catalyzes the reversible conversion of glucose-6-P and glucose-1-P in glycogenolysis and glycogen synthesis (Hers, J *Inherit Metab Dis* 13:395-410, 1990); phosphofructokianse-1 (PFK-1) that catalyzes the irreversible rate-limiting step in glycolysis by converting fructose-6-P to fructose-1,6-diphosphate (Hers, *J Inherit Metab Dis* 13:395-410, 1990); G6P dehydrogenase (G6PDH) that catalyzes the first reaction in the pentose-phosphate pathway by converting G6P to 6-phosphgluconolactone (Wamelink *et al.*, *J Inherit Metab Dis* 31:703-717, 2008); and G6PT that transports cytoplasmic G6P into the ER lumen (Chou *et al.*, *Nat Rev Endocrinol* 6:676-688, 2010).

Quantitative real-time RT-PCR analysis showed that in the fasted livers, PEPCK-C and PGMase transcripts were unchanged while FBPase-1 transcripts were increased in the AAV-GPE-treated G6pc$^{-/-}$ mice, compared to the controls. Both PFK-1 and G6PDH transcripts in AAL-L livers were increased although in AAV-M and AAV-H livers they were still statistically similar to that of wild type livers. Hepatic G6PT mRNA levels in the AAV-GPE-treated G6pc$^{-/-}$ mice were 2.2-fold higher than the wild-type controls, regardless of the levels of hepatic G6Pase-α activity restored. The G6PT-mediated hepatic microsomal G6P uptake activity is the

rate-limiting in endogenous glucose production (Arion *et al.*, *J Biol Chem* 251:6784-690, 1976), but is co-dependent upon G6Pase-α activity (Lei *et al.*, *Nat Genet* 13: 203-209, 1996). Hepatic microsomes prepared from G6pc$^{-/-}$ mice, with an intact G6PT, exhibit markedly lower G6P uptake activity compared to wild type hepatic microsomes (Lei *et al.*, *Nat Genet* 13: 203-209, 1996), which can be reversed if G6Pase-α activity is restored via gene transfer (Zingone *et al.*, *J Biol Chem* 275:828-832, 2000). In AAV-L, AAV-M, and AAV-H livers, microsomal G6P uptake activities were 43%, 50%, and 72%, respectively of wild type activity, reflecting the increase in hepatic G6Pase-α activity (FIG. 2A) that paralleled hepatic free glucose levels.

Absence of immune response against human G6Pase-α

To determine whether a humoral response directed against human G6Pase-α is generated in the infused mice, Western blot analysis was performed using the sera obtained from the 70-90-week-old control and AAV-GPE-treated G6pc$^{-/-}$ mice. A monoclonal antibody against human G6Pase-α that also recognizes murine G6Pase-α (Yiu *et al.*, *Mol Ther* 18:1076-1084, 2010) was used as a positive control. No antibodies directed against G6Pase-α were detected in any of the AAV-GPE-infused G6pc$^{-/-}$ or wild type control mice that lived to age 70 to 90 weeks.

Example 3: The upstream enhancer elements of the *G6PC* promoter are critical for optimal G6PC expression in glycogen storage disease type Ia

This example describes studies to further evaluate the efficacy of the AAV-GPE vector. AAV-GPE, which is a single-stranded vector comprising 2684 bp of the G6PC promoter/enhancer, was compared to AAV-miGPE, a double-stranded vector containing a 382 bp minimal G6PC promoter/enhancer. The results described in this example show that the AAV-GPE vector directed significantly higher levels of hepatic G6Pase-α expression, achieved greater reduction in hepatic glycogen accumulation, and led to a better toleration of fasting in GSD-Ia mice than the AAV-miGPE vector.

MATERIALS AND METHODS

Infusion of G6pc-/- mice with rAAV vectors

All *G6pc-/-* mice were kept alive with glucose therapy (Lei *et al.*, *Nat. Genet.* 13:203-209, 1996). The rAAV vectors were infused into 2-week-old *G6pc-/-* mice via the retro-orbital sinus. Age-matched *G6pc+/+*/*G6pc+/-* mice were used as controls. For rAAV vector-infused mice, glucose therapy was terminated immediately after infusion. All viral transductions were performed on 2-week-old *G6pc-/-* mice and the efficacy evaluated at age 12 weeks.

Phosphohydrolase assays

Microsome isolation and phosphohydrolase assays were determined essentially as described previously (Lei *et al.*, *Nat. Genet.* 13:203-209, 1996). For phosphohydrolase assays, reaction mixtures (100 μl) containing 50 mM cacodylate buffer, pH 6.5, 10 mM G6P and appropriate amounts of microsomal preparations were incubated at 30°C for 10 minutes. Disrupted microsomal membranes were prepared by incubating intact membranes in 0.2% deoxycholate for 20 minutes at 0°C. Non-specific phosphatase activity was estimated by pre-incubating disrupted microsomal preparations at pH 5 for 10 minutes at 37°C, to inactivate the acid labile G6Pase-α.

Quantification of vector DNA and mRNA

Total DNA from mouse tissues was isolated using the GenElute™ Mammalian Genomic DNA Miniprep Kits (Sigma-Aldrich, St Louis, MO) and total RNAs were isolated from mouse tissues using the TRIzol™ Reagent (Invitrogen, Carlsbad, CA). The vector genome numbers and mRNA expression were quantified by PCR and real-time RT-PCR, respectively in an Applied Biosystems 7300 Real-Time PCR System using Applied Biosystems TaqMan probes (Applied Biosystems, Foster City, CA). The vector genome numbers of human *G6PC* gene was normalized to mouse β-actin using TaqMan probe sets Hs00609178_m1 for *G6PC* and Mm00607939_s1 for β-actin. Plasmid DNA corresponding to 0.01 to 100 copies of human *G6PC* gene was used in a standard curve. To determine the vector genome copy number, the Ct values of sample were compared to the standard curve. G6PC mRNA expression was normalized to Rpl19 RNA using TaqMan® probe sets Hs00609178_m1 for G6PC and Mm02601633_g1 for Rpl19.

Phenotype analyses

Blood glucose was analyzed using kits obtained from Thermo Electron (Louisville, CO). Hepatic glycogen and triglyceride contents were measured as described previously (see Examples 1 and 2, and Yiu *et al.*, *Mol. Ther.* 18:1076-1084, 2010; Lee *et al.*, *Hepatology* 56:1719-1729, 2012). To determine hepatic triglyceride, liver tissues were homogenized in RIPA buffer (50 mM Tris HCl, pH 8.0, 150 mM NaCl, 1% Triton X-100, 0.5% Na-deoxycholate, and 0.1% SDS) (Thermo Scientific, Rockford, IL), and triglycerides were measured using a kit from Sigma Diagnostics (St Louis, MO).

Glucose tolerance testing of mice consisted of fasting for 6 hours, prior to blood sampling, followed by intraperitoneal injection of a glucose solution at 2 mg/g body weight, and repeated blood sampling via the tail vein for 2 hours.

Statistical analysis

The unpaired t test was performed using the GraphPad Prism® Program, version 4 (GraphPad Software Inc., San Diego, CA). Values were considered statistically significant at $p < 0.05$.

RESULTS

Hepatic G6Pase-α expression in rAAV-GPE- or rAAV-miGPE-treated G6pc-/- mice

Studies were conducted to examine the efficacy of the rAAV-GPE (see Example 1 and Yiu *et al.*, *Mol. Ther.* 18:1076-1084, 2010) and rAAV-miGPE (Koeberl *et al.*, *Mol. Ther.* 16:665-672, 2008) vectors in treating *G6pc-/-* mice over 12-weeks. Each vector was used at two doses, 1 x 10^{13} viral particles (vp)/kg (high dose) and 2 x 10^{12} vp/kg (low dose) with 6 mice per group, at two different research centers. Similar results were obtained from both centers. While hepatic G6Pase-α activity in the transduced *G6pc-/-* mice represents the combined data from the two centers, other reported data are from a single study. Studies have shown that the efficiency and persistence of rAAV-mediated hepatic gene transfer are lower during early development because of the fast rate of hepatocellular proliferation associated with liver growth, which dilutes out the number of cells effectively infected with rAAV (Yiu *et al.*, *Mol. Ther.* 18:1076-1084, 2010; Cunningham, *Mol. Ther.* 16:1081-1088, 2008). In this study, the rAAV vectors were administered to 2-week-old *G6pc-/-* mice when hepatocellular proliferation remains high. Consequently, hepatic G6Pase-α expression examined at age 12 weeks is significantly lower than that seen in adult mice infused with the same vector dosage. The best time of intervention in the human disease remains to be established.

All treated *G6pc-/-* mice survived to age 12 weeks with no premature deaths at either center. In the liver of 12-week-old wild type mice, microsomal G6Pase-α activity was 203.5 ± 10.3 nmol/min/mg (n = 24). The combined data (n = 12 per treatment), determined independently at the two centers, showed that at age 12 weeks, the high dose rAAV-GPE therapy reconstituted about 18% of wild type hepatic G6Pase-α activity which was 3.5-fold more activity than rAAV-miGPE, while the low dose rAAV-GPE therapy produced over 3.6 times more activity than rAAV-miGPE (FIG. 6A). The hepatic G6Pase-α activity increased linearly with hepatic vector genome copy

number, and the copy numbers in rAAV-GPE-treated *G6pc-/-* mice (n = 6) were significantly higher than the rAAV-miGPE-treated mice (n = 6) (FIG. 6A).

Metabolic profiles of rAAV-GPE- or rAAV-miGPE-treated G6pc-/- mice

All rAAV-GPE- and rAAV-miGPE-treated *G6pc-/-* mice exhibited growth curves that paralleled their wild type littermates, albeit at lower weights (FIG. 6B). The body mass index (BMI) values of the treated mice were indistinguishable from those of wild type mice irrespective of the vector or dose level (FIG. 6C). All treated *G6pc-/-* mice had blood glucose levels consistently lower than wild type controls, but still above the lower end of the normal range (FIG. 6D), and none of the infused animals suffered from the frequent hypoglycemic seizures typical of GSD-Ia (Chou *et al.*, *Curr. Mol. Med.* 2:121-143, 2002; Chou *et al.*, *Nat. Rev. Endocrinol.* 6: 676-688, 2010; Lee *et al.*, *Hepatology* 56:1719-1729, 2012).

The relative weight of the liver to the body, one measure of liver glycogen and/or neutral fat accumulation (Chou *et al.*, *Curr. Mol. Med.* 2:121-143, 2002; Chou *et al.*, *Nat. Rev. Endocrinol.* 6: 676-688, 2010), was higher in all 4 treated *G6pc-/-* mouse groups than wild type mice, although the high dose rAAV-GPE-treated mice were significantly closer to normal than the other groups (FIG. 7A). Consistent with this, glycogen contents in rAAV-GPE- and rAAV-miGPE-treated *G6pc-/-* mice were markedly higher than their wild type controls (FIG. 7B) with the higher vector doses lowering glycogen better than the lower vector doses, demonstrating that restoring higher hepatic G6Pase-α expression improves hepatomegaly. However, comparing just high dose therapies, the rAAV-miGPE-treated mice had 43% more glycogen than rAAV-GPE-treated mice. Despite the continued elevation in liver glycogen there were no histological abnormalities observed in the liver tissue sections of any of the rAAV-treated *G6pc-/-* mice at age 12 weeks. With the exception of rAAV-miGPE-treated mice at a low dose, hepatic triglyceride contents were not statistically different between wild type and the other 3 groups of rAAV-treated *G6pc-/-* mice (FIG. 7C).

Fasting glucose and glucose tolerance profiles in rAAV-GPE- or rAAV-miGPE-treated G6pc-/- mice

For wild type mice (n = 24), the mean blood glucose level before fasting was 172.2 ± 2.6 mg/dl (zero time), which decreased to 134.6 ± 3.8 mg/dl after 8 hours of fast (FIG. 8A). The fasting blood glucose profiles of high dose therapy mice (n = 6 per treatment) were significantly better than low dose therapy mice (n = 6 per treatment), however, even at high dose, rAAV-GPE-treated mice sustained significantly higher glucose levels that stabilized to wild type levels

6 hours into the fast, while rAAV-miGPE-treated mice plateaued much lower at 60% of wild type levels (FIG. 8A). The high dose rAAV-GPE- and rAAV-miGPE-treated mice could also sustain a 24-hour fast but fasting blood glucose levels were significantly higher in rAAV-GPE-treated mice than rAAV-miGPE-treated mice (FIG. 8B). In summary, the rAAV-GPE-treated *G6pc-/-* mice were closer to wild type and more capable of tolerating fasting than the rAAV-miGPE-treated *G6pc-/-* mice.

Blood glucose tolerance profiles of the treated *G6pc-/-* mice (n = 6 per treatment) were monitored following an intraperitoneal glucose injection. In general, the profiles paralleled those of the wild-type mice (FIG. 8C) with the high dose treated mice responding better than the low dose treated mice.

The bio-distribution of the human *G6PC* transgene in liver, kidney, intestine, brain, testis, and ovary in 12-week-old, high dose rAAV-GPE-treated *G6pc-/-* mice was analyzed by quantitative PCR (Table 1). In the transduced liver, vector genome copy numbers/μg DNA was 94,440 ± 7,624 (or 0.51 ± 0.04 vector copies/diploid genome). In the transduced kidney and intestine, the numbers were dramatically lower, averaging just 2.57% and 0.64% respectively of liver copy number, showing that the rAAV8 virus did not transduce kidney and intestine efficiently. The genome copy numbers/μg DNA in the brain and testis were even lower at 0.12% and 0.02%, respectively of liver copy number. Only background levels of human *G6PC* genomes were detected in the ovary.

The rAAV-GPE vector contains a tissue-specific promoter/enhancer element expressed primarily in the liver, proximal tubules in the kidney, and intestine (Chou *et al.*, *Curr. Mol. Med.* 2:121-143, 2002; Chou *et al.*, *Nat. Rev. Endocrinol.* 6: 676-688, 2010). Quantitative real-time RT-PCR analysis of human G6PC transcripts showed a correlation between genome copy number and gene expression (Table 3). In the liver, levels of human G6PC mRNA relative to the RpI19 transcript were 0.62740 ± 0.04445. As expected from the genome copy analysis, the kidney expressed only 0.03% of the liver human G6PC mRNA, and only background levels of human G6PC mRNA were detected in the intestine, brain, testis, and ovary.

Table 3. Human *G6PC* genome distribution and mRNA expression in 12-week-old high dose rAAV-GPE-treated *G6pc-/-* mice

Tissue	Human G6PC Copy number/μg genomic DNA	Human G6PC mRNA relative to RpI19 mRNA × 10^5
Wild type tissues, no transgene (n = 6)	8 ± 2	8 ± 1
Liver, -/-/rAAV-GPE (n = 6)	94,440 ± 7,624 (100)	62740 ± 4445 (100)

Tissue	Human G6PC Copy number/μg genomic DNA	Human G6PC mRNA relative to RpI19 mRNA $\times 10^5$
Kidney, -/-/rAAV-GPE (n = 6)	2,429 ± 626 (2.57)	22 ± 5 (0.033)
Intestine, -/-/rAAV-GPE (n = 6)	601 ± 124 (0.64)	9 ± 1
Brain, -/-/rAAV-GPE (n = 6)	121 ± 23 (0.12)	8 ± 1
Testis, -/-/rAAV-GPE (n = 6)	25 ± 8 (0.02)	9 ± 1
Ovary, -/-/rAAV-GPE (n = 6)	7 ± 2	9 ± 1

Data are means ± SEM. The values of wild type tissues, which contain no transgene, were the mean ± SEM of liver, kidney, intestine, brain, testis, and ovary. Numbers in parentheses are % of liver value.

Example 4: Comparison of AAV vectors with and without stuffer sequences

This example describes the finding that the stuffer nucleotide sequence flanking the intron in G6Pase-α-expressing AAV vectors is important for efficient hepatic transduction.

To evaluate the contribution of the stuffer sequence to transgene delivery and hepatic expression of G6Pase-α, plasmid UF11-K29-G6PC was constructed. UF11-K29-G6PC (SEQ ID NO: 2) differs from UF11-GPE-G6PC (SEQ ID NO: 1) in lacking the stuffer sequence around the intron. The G6PC promoter/enhancer (GPE) and the G6PC coding sequences are identical in each plasmid.

G6pc-/- mice were administered 1 x 10^{13} vp/kg of either recombinant AAV-K29-G6PC or recombinant AAV-GPE-G6PC. The results indicated that AAV-K29-G6PC exhibited markedly reduced hepatic transducing efficiency in GSD-Ia mice, compared to AAV-GPE-G6PC. G6Pase activities in AAV-K29-G6PC- and AAV-GPE-G6PC-transduced liver were 7.3 and 33.0 nmol/min/mg, respectively. These results demonstrate that the stuffer sequence flanking the intron is important for efficient hepatic transduction.

Example 5: Generation of an AAV vector encoding codon-optimized G6PC

This example describes the construction and characterization of an AAV vector containing codon-optimized G6PC.

The UF11-GPE-co-G6PC plasmid (comprising codon-optimized G6PC; SEQ ID NO: 3) was derived from the UF11-GPE-G6PC plasmid (SEQ ID NO: 1), but the wild type G6Pase coding sequence in AAV-GPE-G6PC was replaced with a synthetic codon-optimized G6Pase (nucleotides 3368-4441 of SEQ ID NO: 3).

Transient *in vitro* expression assays showed that co-G6Pase exhibited enzyme activity 1.9-fold higher than wild type human G6Pase. In addition, two batches of recombinant AAV-GPE-co-G6PC have been evaluated for *in vivo* activity and compared to the activity of recombinant AAV-GPE-G6PC in GSD-Ia mice. The first batch of AAV-GPE-co-G6PC was 50% more efficient than AAV-GPE-G6PC in transducing the liver than AAV-GPE-G6PC. The second batch of AAV-GPE-co-G6PC was 2.5-fold more efficient in transducing the liver than recombinant AAV-GPE-G6PC.

These results demonstrate that codon-optimization of G6PC increases the liver transduction capacity of recombinant AAV expressing G6Pase-α.

Example 6: Evaluation of the efficacy of a recombinant AAV vector expressing codon-optimized human G6Pase

The example describes a study to compare the efficacy of gene delivery mediated by rAAV8-GPE-G6Pase and rAAV8-GPE-co-G6Pase in GSD-Ia mice.

The efficacy of gene delivery in GSD-Ia mice was compared using 2-3 independent batches of two AAV vectors: 1) rAAV8-GPE-G6Pase (a rAAV8 vector expressing human G6Pase-α directed by the ~3kb human G6PC promoter/enhancer (GPE); and 2) rAAV8-GPE-co-G6Pase (a rAAV8 vector expressing a codon-optimized (co) human G6Pase-α directed by the GPE). The results in FIG. 11 show that hepatic G6Pase activities in both 4- and 12-week-old rAAV8-GPE-co-hG6Pase-treated GSD-Ia mice were 1.9-fold higher than the respective activities restored by the rAAV8-GPE-G6Pase vector.

All treated GSD-Ia mice exhibited normal serum profiles of cholesterol, triglyceride, uric acid and lactic acid and normal levels of hepatic fat. In rAAV-infused mice, liver weights were inversely correlated to the hepatic G6Pase activity restored. The rAAV-GPE-G6Pase-treated mice exhibited significantly more severe hepatomegaly as compared to the rAAV-GPE-co-G6Pase-treated mice (FIG. 12).

Functionally, at age 12 weeks, the rAAV8-GPE-co-G6Pase-treated GSD-Ia mice displayed normal glucose tolerance profiles (FIG. 13A) and maintained normoglycemia over a 24-hour fast (FIG. 13B).

Example 7: Treatment of human GSD-Ia using AAV-based gene therapy

This example describes an exemplary method for the clinical use of AAV vectors encoding G6PC for the treatment of GSD-Ia.

A patient diagnosed with GSD-Ia is selected for treatment. Typically the patient is at least 18 years old and may or may not have had pre-exposure to immunomodulation. The patient is administered a therapeutically effective amount of a recombinant AAV expressing G6PC, such as AAV-GPE-G6PC or AAV-GPE-co-G6PC as disclosed herein. The recombinant AAV can be administered intravenously. An appropriate therapeutic dose can be selected by a medical practitioner. In some cases, the therapeutically effective dose is in the range of 1×10^{11} to 1×10^{14} viral particles (vp)/kg, such as about 1×10^{12} vp/kg. In most instances, the patient is administered a single dose. In the absence of immunomodulation, the patient is likely to tolerate only a single infusion of rAAV. If the subject has had pre-exposure immunomodulation, two or more doses may be administered. The health of the subject can be monitored over time to determine the effectiveness of the treatment.

In view of the many possible embodiments to which the principles of the disclosed invention may be applied, it should be recognized that the illustrated embodiments are only preferred examples of the invention and should not be taken as limiting the scope of the invention. Rather, the scope of the invention is defined by the following claims. We therefore claim as our invention all that comes within the scope and spirit of these claims.

CLAIMS:

1. A recombinant nucleic acid molecule comprising nucleotides 182-4441 of SEQ ID NO: 3 or nucleotides 182-4441 of SEQ ID NO: 1.

2. The recombinant nucleic acid molecule of claim 1, comprising nucleotides 17-4819 of SEQ ID NO: 3 or nucleotides 17-4819 of SEQ ID NO: 1.

3. The recombinant nucleic acid molecule of claim 1 or claim 2, comprising the nucleotide sequence of SEQ ID NO: 3 or SEQ ID NO: 1.

4. A vector comprising the recombinant nucleic acid molecule of any one of claims 1-3.

5. The vector of claim 4, wherein the vector is an adeno-associated virus (AAV) vector.

6. The vector of claim 5, wherein the AAV vector is an AAV serotype 8 (AAV8) vector.

7. An isolated host cell comprising the recombinant nucleic acid molecule of any one of claims 1-3, or the vector of any one of claims 4-6.

8. A recombinant AAV (rAAV) comprising the recombinant nucleic acid molecule of any one of claims 1-3.

9. The rAAV of claim 8, wherein the rAAV is rAAV8.

10. A composition comprising the rAAV of claim 8 or claim 9 in a pharmaceutically acceptable carrier.

11. The composition of claim 10 formulated for intravenous administration.

12. Use of a therapeutically effective amount of the rAAV of claim 8 or claim 9, or the composition of claim 10 or claim 11, for treating a subject diagnosed with a glycogen storage disease.

13. The use of claim 12, wherein the subject is diagnosed with glycogen storage disease type Ia (GSD-Ia).

Date Reçue/Date Received 2021-04-06

14. The use of claim 12 or claim 13, wherein the rAAV is for intravenous administration.

15. The use of any one of claims 12-14, wherein the rAAV is for administration at a dose of about 1 x 10^{11} to about 1 x 10^{14} viral particles (vp)/kg.

16. The use of claim 15, wherein the rAAV is for administration at a dose of about 1 x 10^{12} to 8 x 10^{13} vp/kg.

17. The use of claim 15, wherein the rAAV is for administration at a dose of about 1 x 10^{13} to 6 x 10^{13} vp/kg.

18. The use of any one of claims 12-17, wherein the rAAV is for administration in a single dose.

19. The use of any one of claims 12-17, wherein rAAV is for administration in multiple doses.

Date Reçue/Date Received 2021-04-06

FIG. 1A

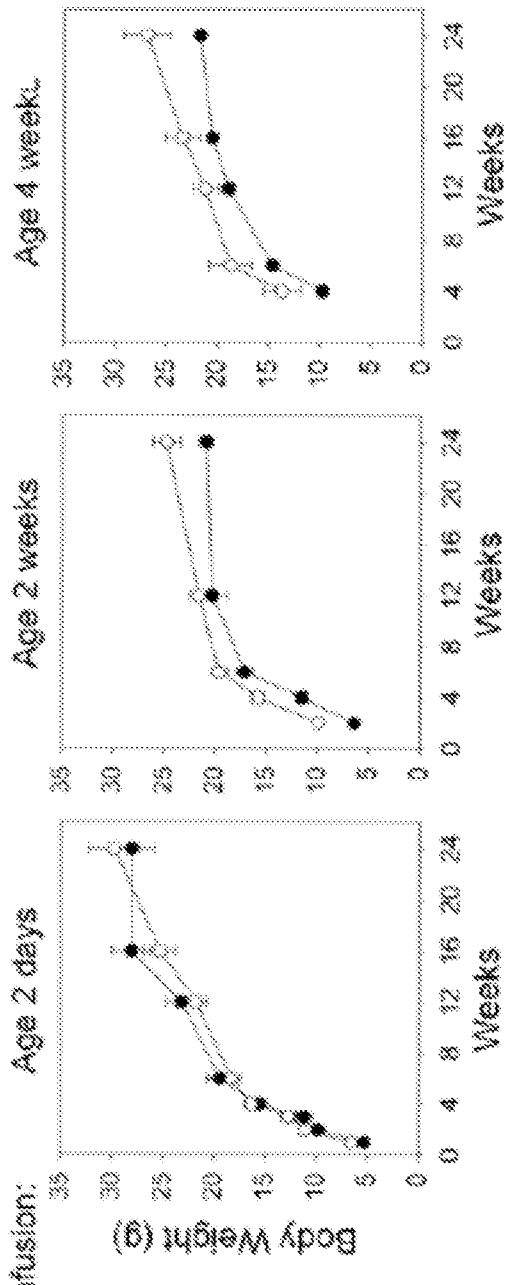
Infusion:
Age 2 days
Age 2 weeks
Age 4 weeks
Body Weight (g)
Weeks

FIG. 1B

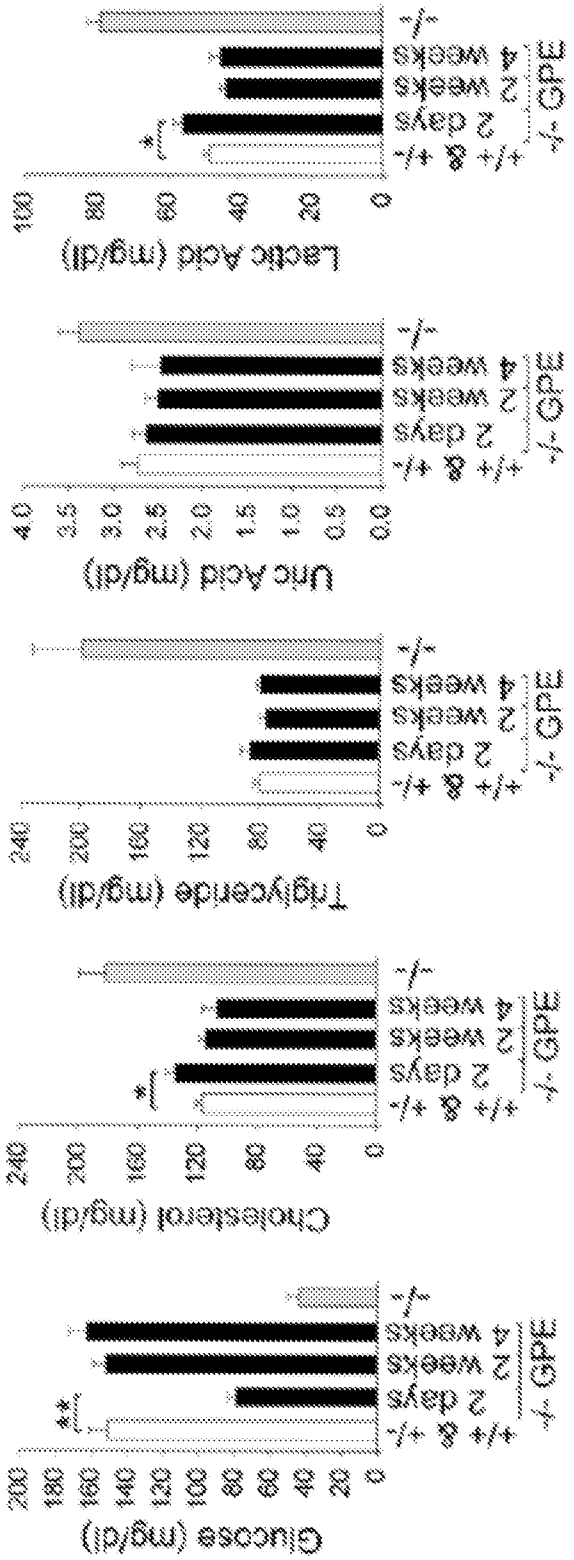
Glucose (mg/dl)
Cholesterol (mg/dl)
Triglyceride (mg/dl)
Uric Acid (mg/dl)
Lactic Acid (mg/dl)
+/+ & +/-
2 days
2 weeks
4 weeks
-/-
+/- GPE

FIG. 2A

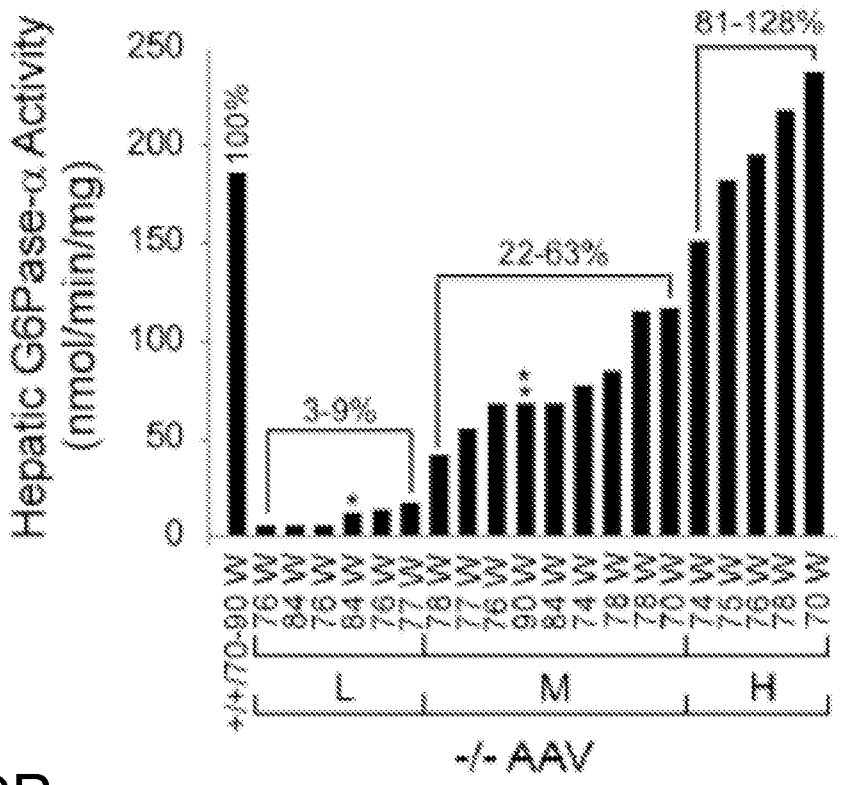
Hepatic G6Pase-α Activity
(nmol/min/mg)
250
200
150
100
50
0
100%
3-9%
22-63%
81-128%
*
**
+/+ 70-90 W
-/- AAV
L
M
H

FIG. 2B

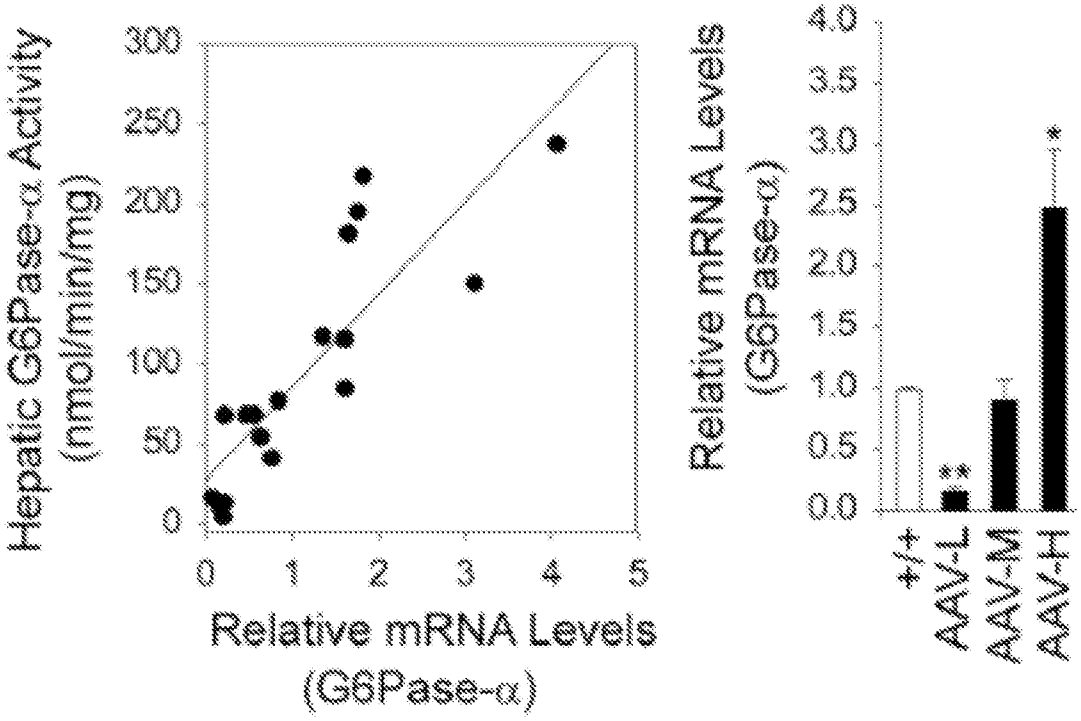
Hepatic G6Pase-α Activity
(nmol/min/mg)
300
250
200
150
100
50
0
0 1 2 3 4 5
Relative mRNA Levels
(G6Pase-α)
Relative mRNA Levels
(G6Pase-α)
4.0
3.5
3.0
2.5
2.0
1.5
1.0
0.5
0.0
**
*
+/+
AAV-L
AAV-M
AAV-H

FIG. 3A

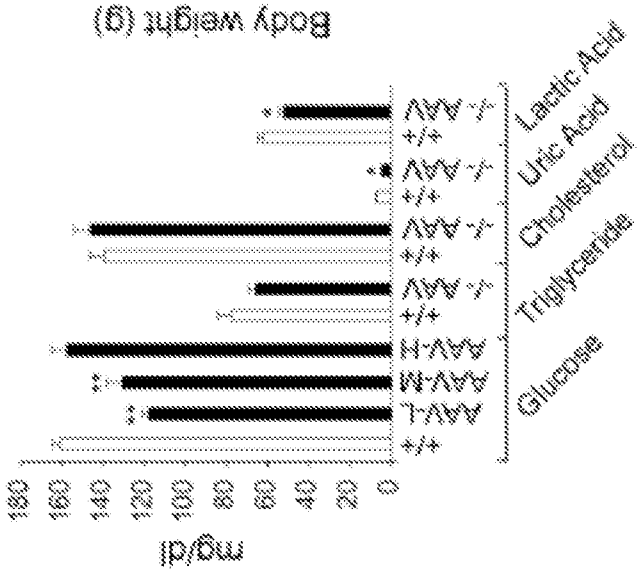

FIG. 3B

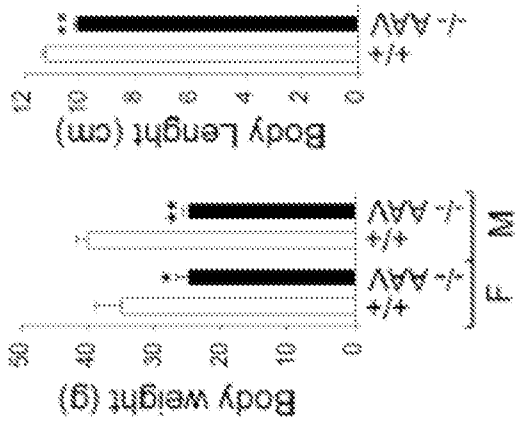

FIG. 3C

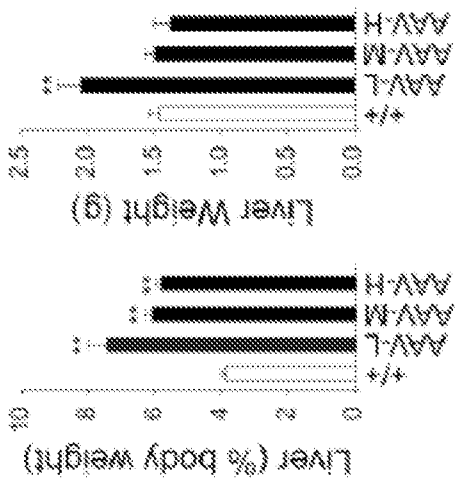

FIG. 4C

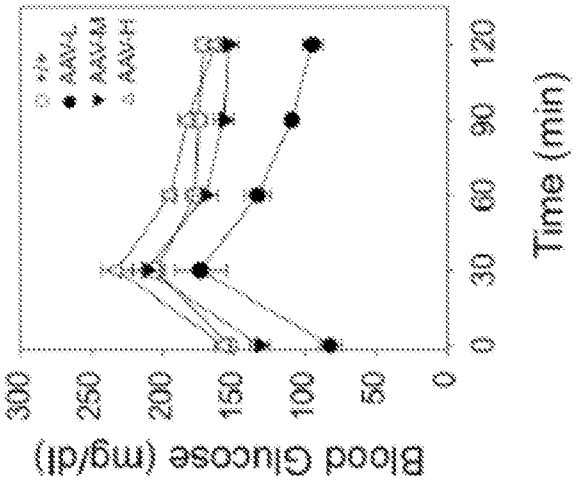

FIG. 4B

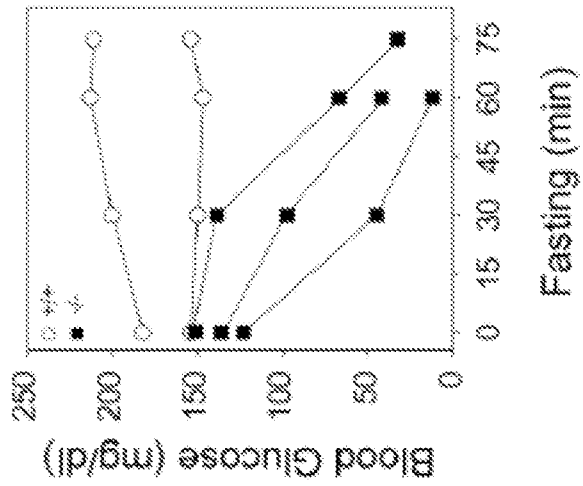

FIG. 4A

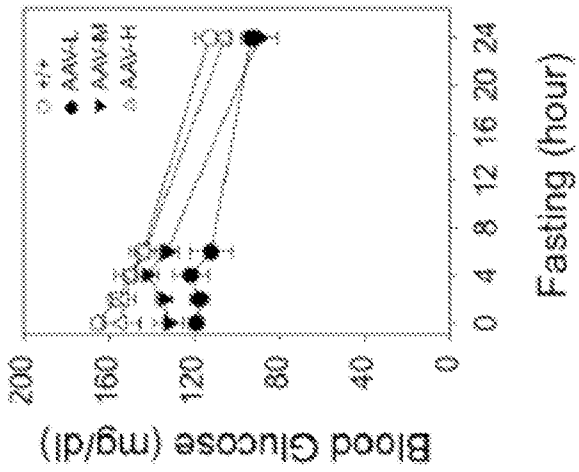

FIG. 5A

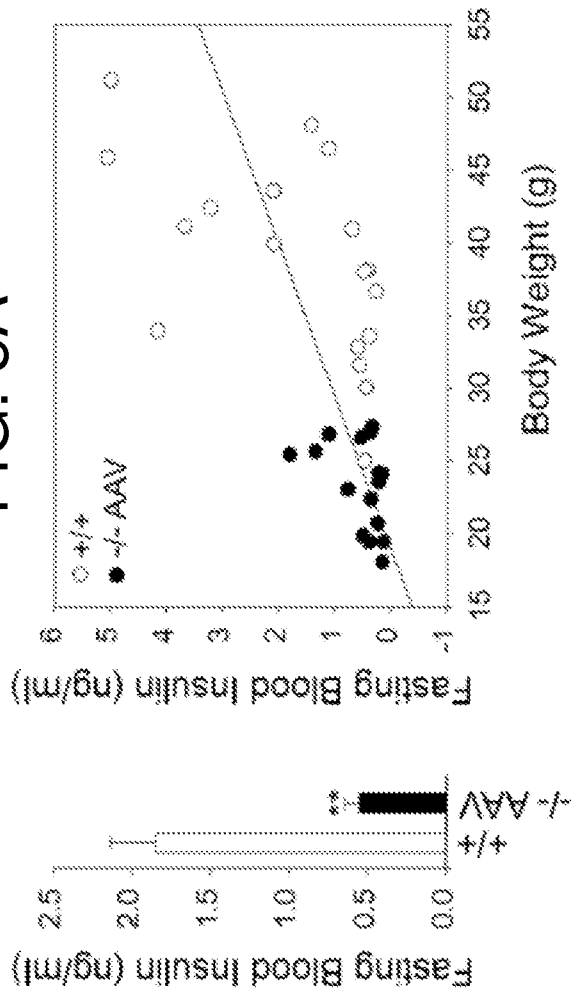

FIG. 5B

FIG. 5C

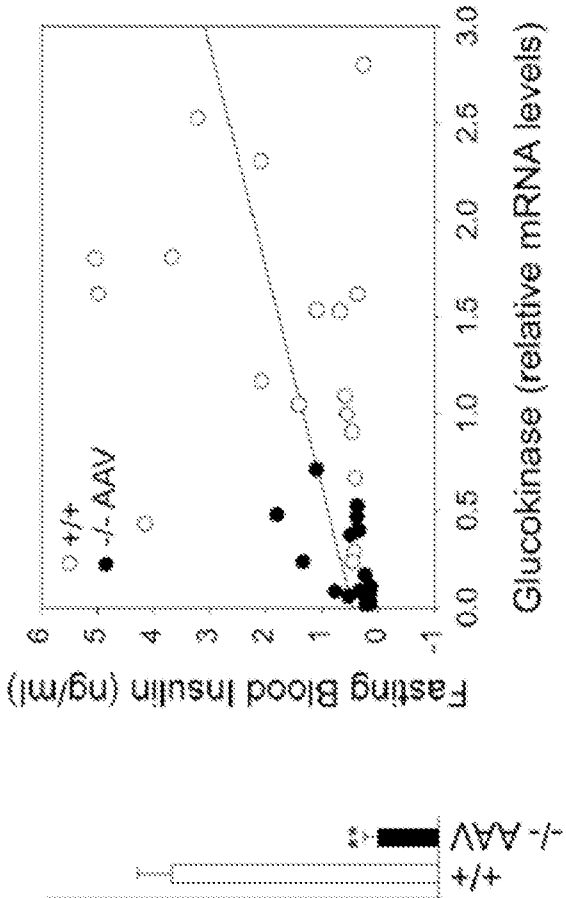

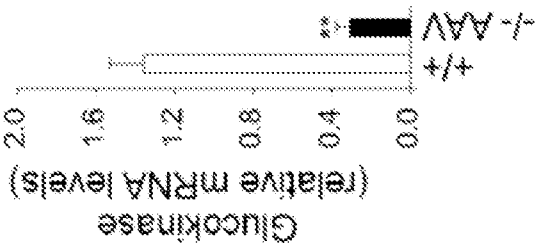

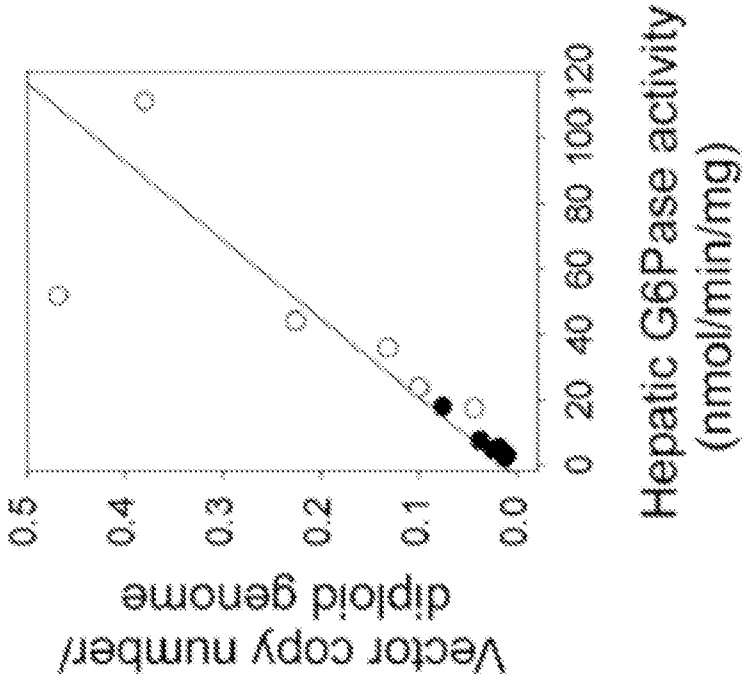
Hepatic G6Pase activity
(nmol/min/mg)
0 20 40 60 80 100 120
Vector copy number/
diploid genome
0.5 0.4 0.3 0.2 0.1 0.0

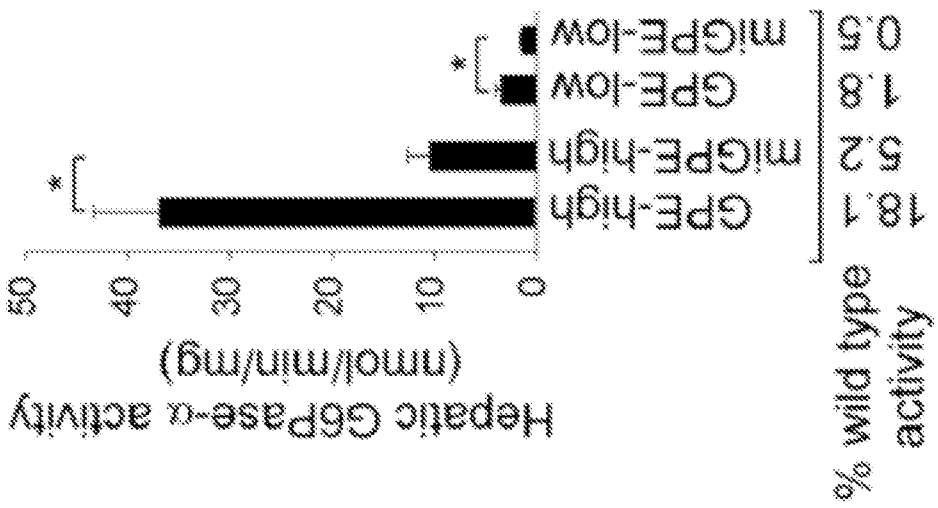
Hepatic G6Pase-α activity
(nmol/min/mg)
60 40 30 20 10 0
*
*
GPE-high
miGPE-high
GPE-low
miGPE-low
% wild type
activity
18.1
5.2
1.8
0.5

FIG. 6A

FIG. 6D

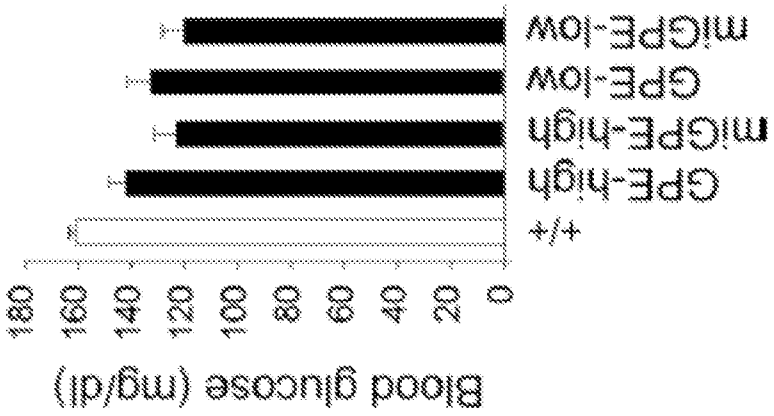

FIG. 6C

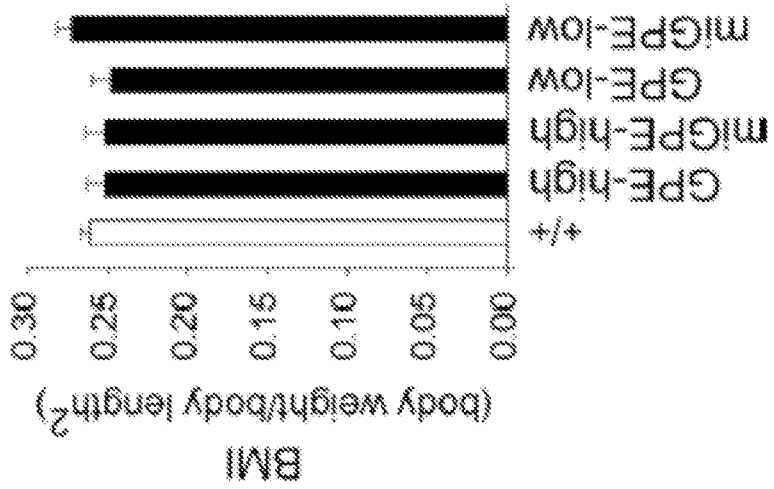

FIG. 6B

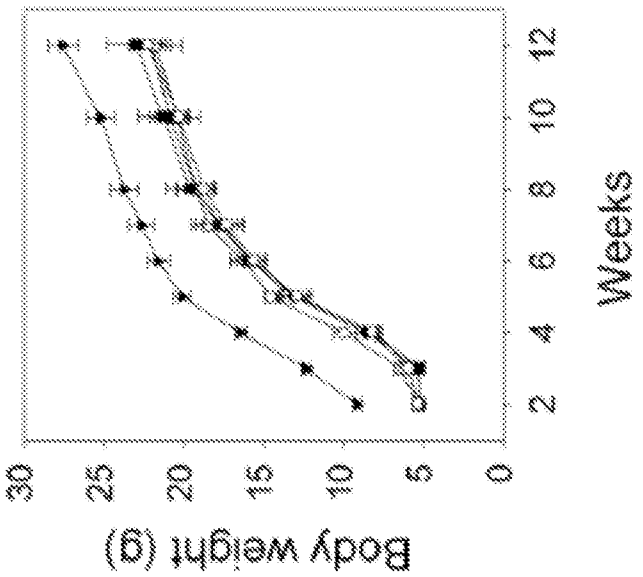

FIG. 7C

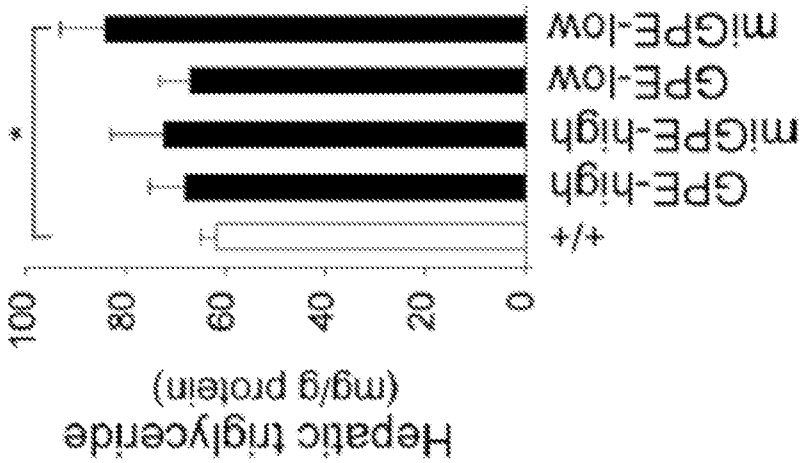

FIG. 7B

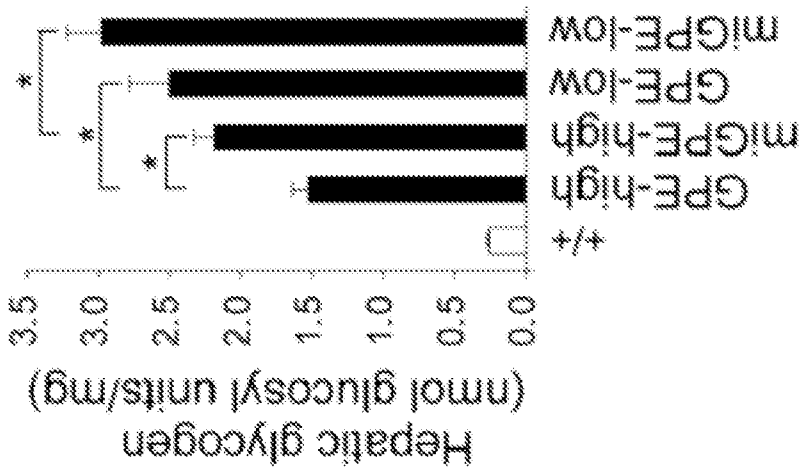

FIG. 7A

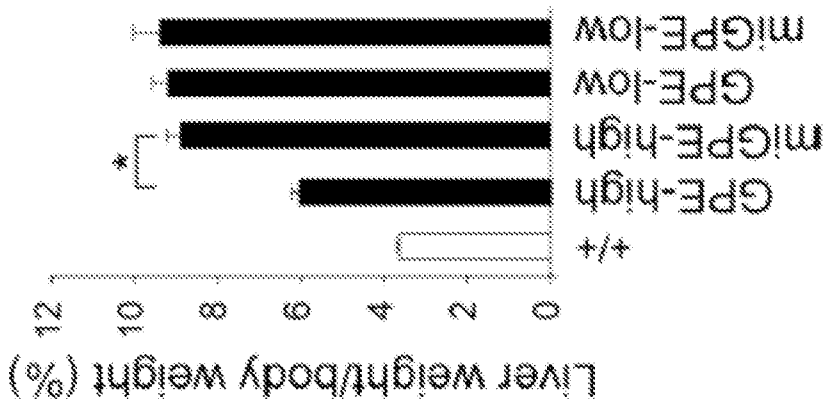

FIG. 8A

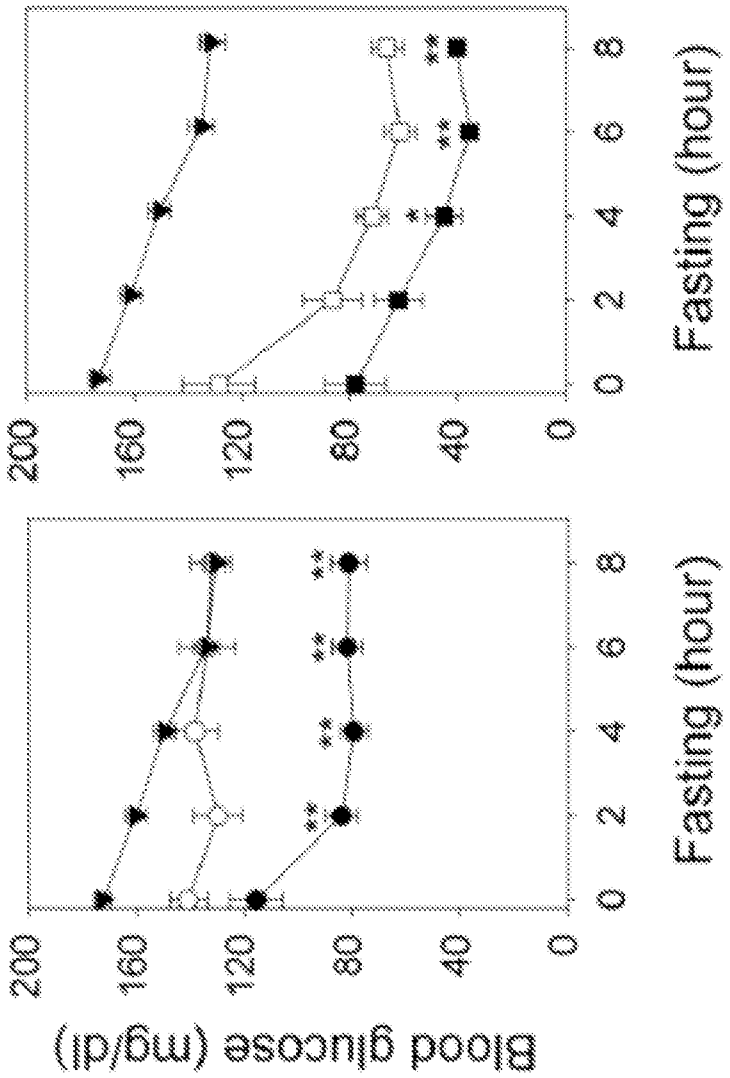
Blood glucose (mg/dl)
200
160
120
80
40
0
0 2 4 6 8
Fasting (hour)
**
**
**
**
200
160
120
80
40
0
0 2 4 6 8
Fasting (hour)
**
**
*
*

FIG. 8B

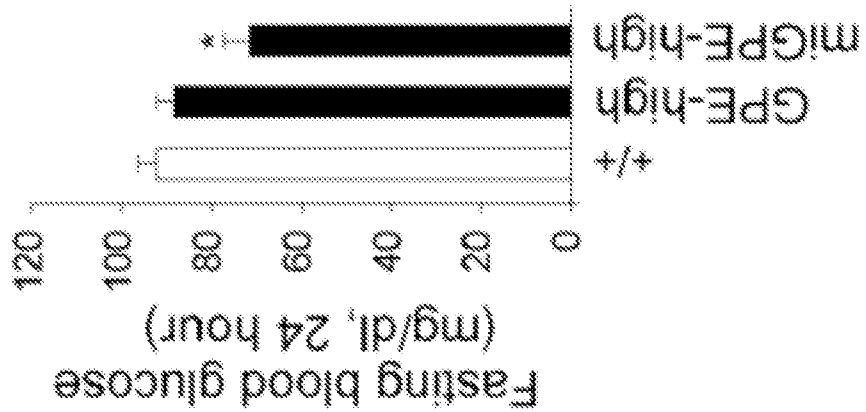
Fasting blood glucose
(mg/dl, 24 hour)
120
100
80
60
40
20
0
+/+
GPE-high
miGPE-high
*

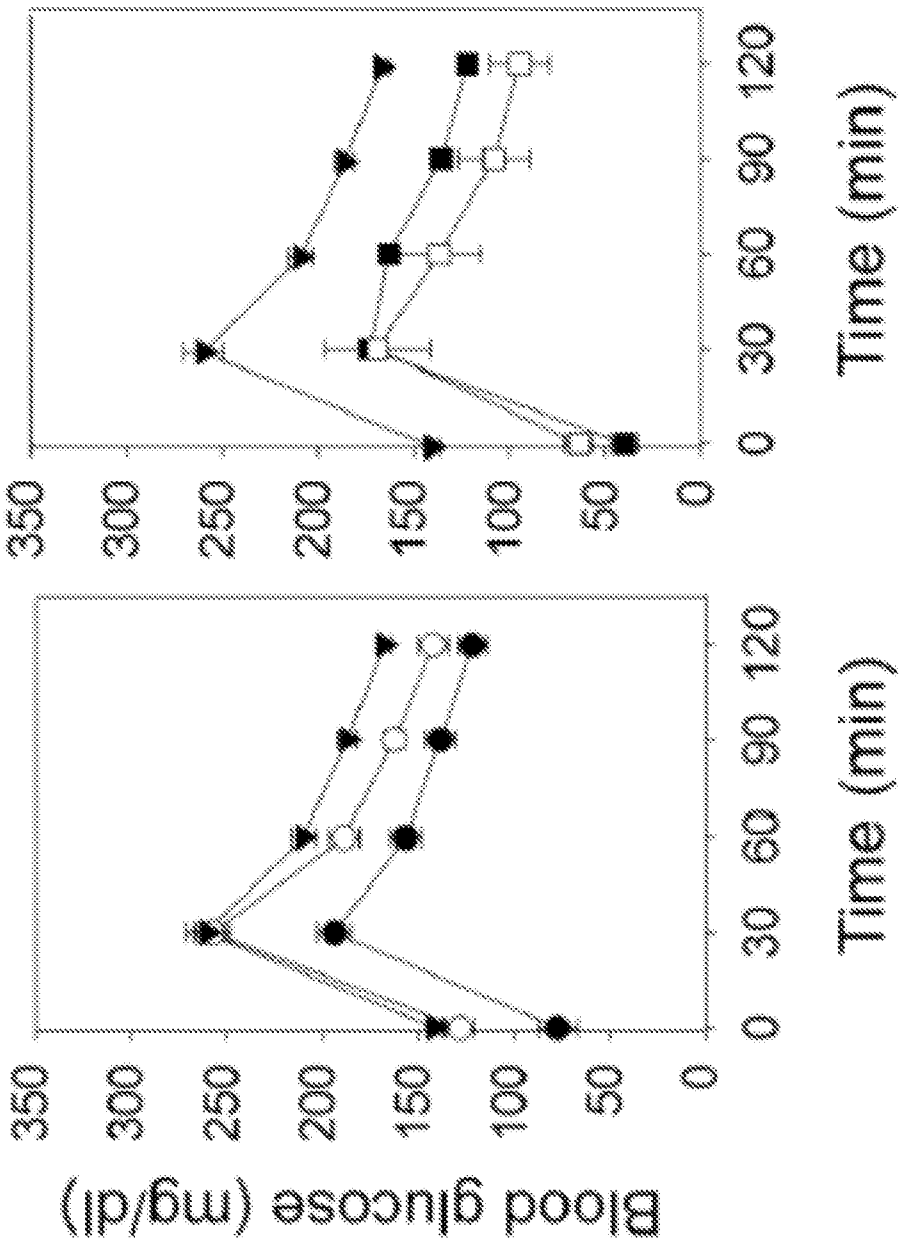
Blood glucose (mg/dl)
350
300
250
200
150
100
50
0
0
30
60
90
120
Time (min)
350
300
250
200
150
100
50
0
0
30
60
90
120
Time (min)

FIG. 8C

FIG. 9

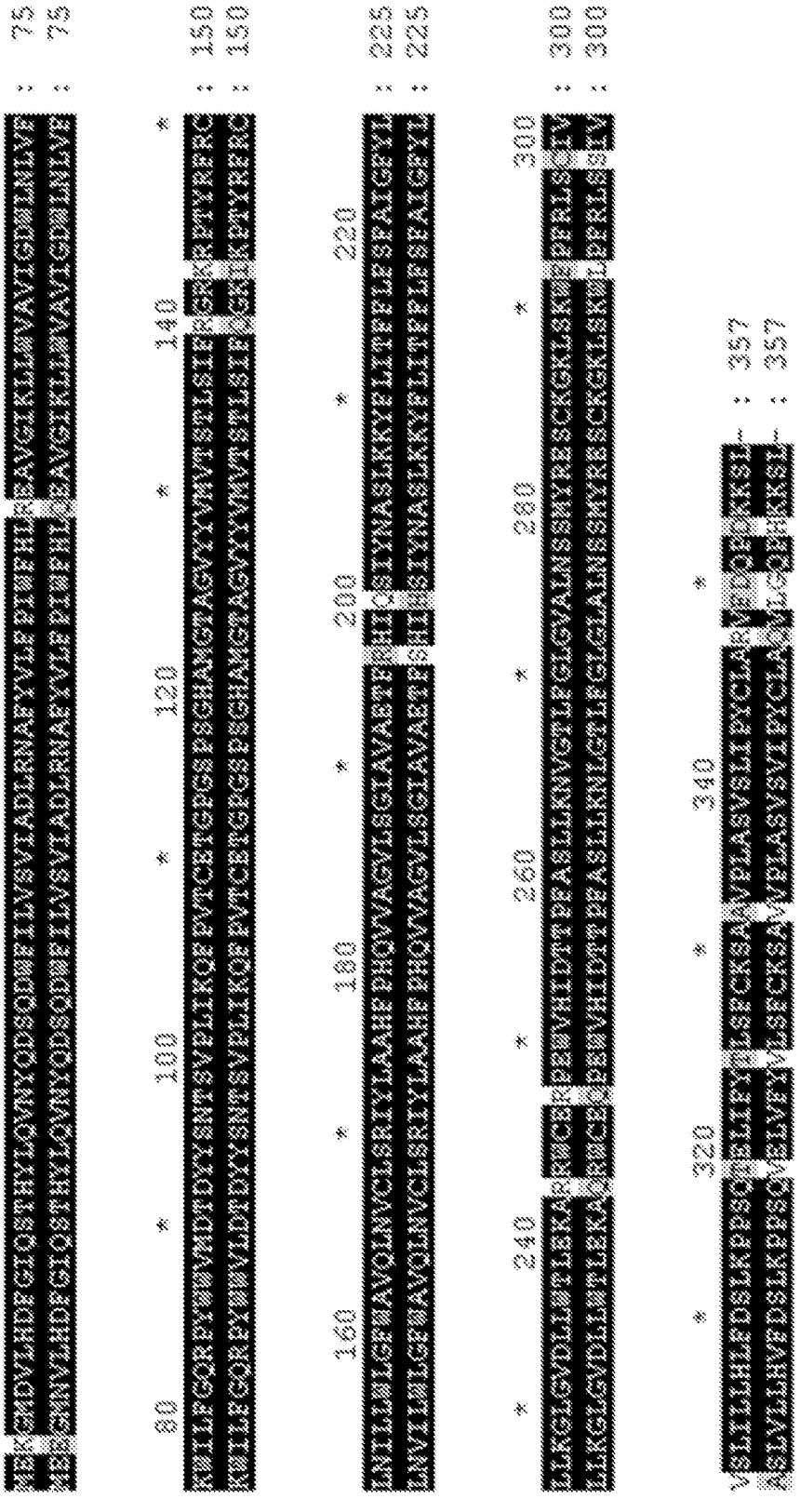

First line: **canine G6Pase-α**
Second line: **human G6Pase-α**

FIG. 10

Amino acid difference between human, mouse, rat and canine G6Pase-α:

	Amino acid	Amino acid	Amino acid	Amino acid	Amino acid	Amino acid	Amino acid	Amino acid
Human	E3 (N)	Q54 (C1)	Q139 (C2)	S196 (H5)	H199 (C3)	Q242 (L3)	Q247 (L3)	L292 (H8)
mouse	E3	K54	R139	S196	H199	K242	R247	F292
Rat	E3	Q54	R139	S196	H199	K242	R247	L292
Dog	**K3**	**R54**	**R139**	**R196**	**Q199**	R242	**R247**	F292
	Amino acid	Amino acid	Amino acid	Amino acid	Amino acid	Amino acid	Amino acid	Amino acid
Human	S298 (H8)	A301 (H8)	V318 (L4)	V324 (H9)	V332 (H9)	Q347 (C)	L349 (C)	G350 (C)
mouse	C298	A301	V318	I324	T332	R347	L349	G350
Rat	C298	A301	I318	I324	T332	R347	L349	G350
Dog	**C298**	**V301**	**T318**	**T324**	**A332**	R347	**F349**	**D350**
	Amino acid	Amino acid	Amino acid	Amino acid	Amino acid	Amino acid	Amino acid	Amino acid
Human	H353 (C)							
mouse	H353							
Rat	H353							
Dog	**D353**							

H: helical domain (H1 to H9)
N- N-terminal domain
C: carboxyl terminal domain
L-loop: luminal loop (L1 to L4)
C-loop: cytoplasmic loop (C1 to C4)

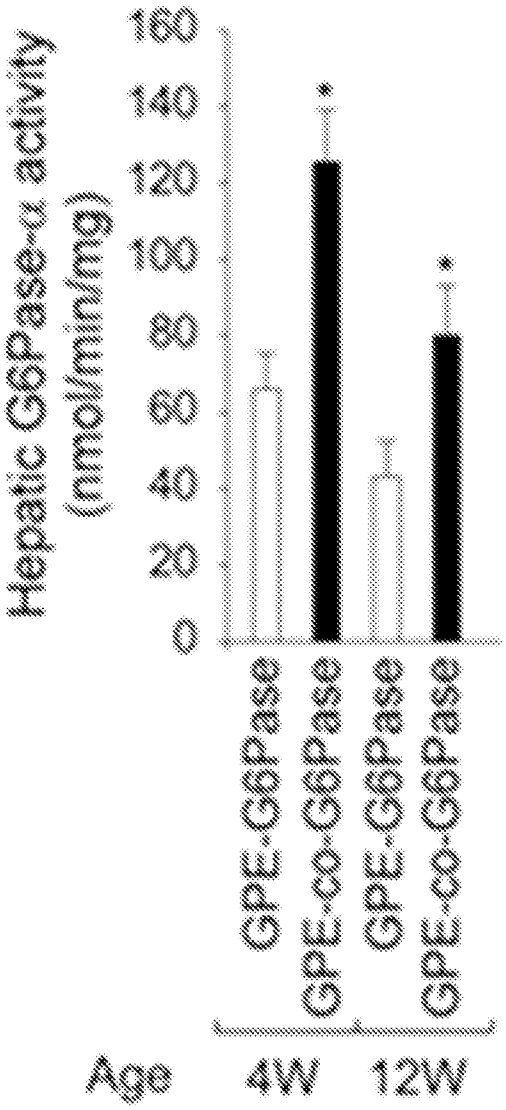
Hepatic G6Pase-α activity
(nmol/min/mg)
160
140
120
100
80
60
40
20
0
*
*
GPE-G6Pase
GPE-cO-G6Pase
GPE-G6Pase
GPE-cO-G6Pase
Age
4W
12W

FIG. 11

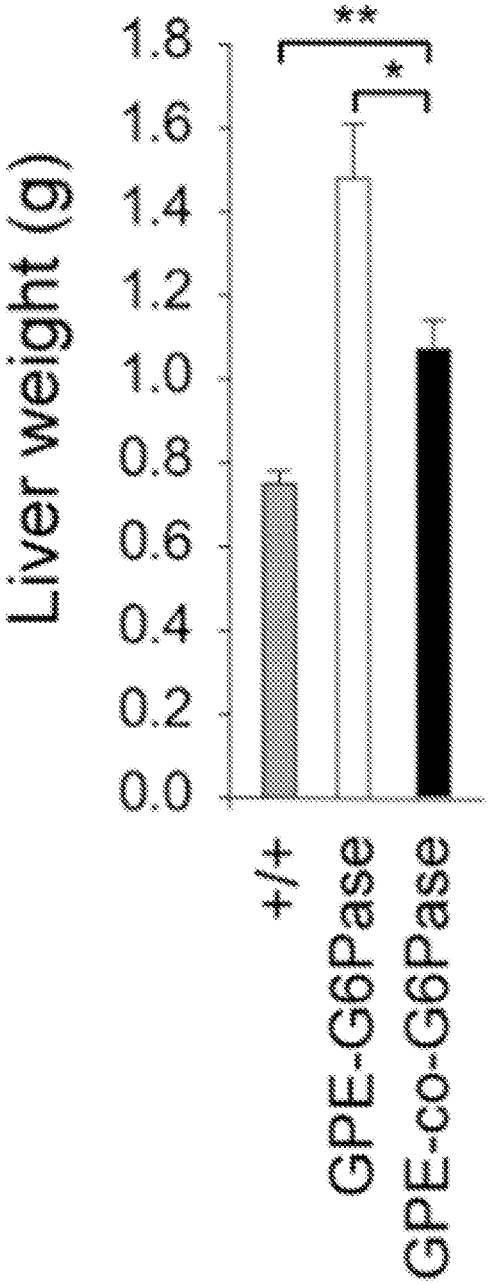
Liver weight (g)
1.8
1.6
1.4
1.2
1.0
0.8
0.6
0.4
0.2
0.0
**
*
+/+
GPE-G6Pase
GPE-co-G6Pase

FIG. 12

FIG. 13A

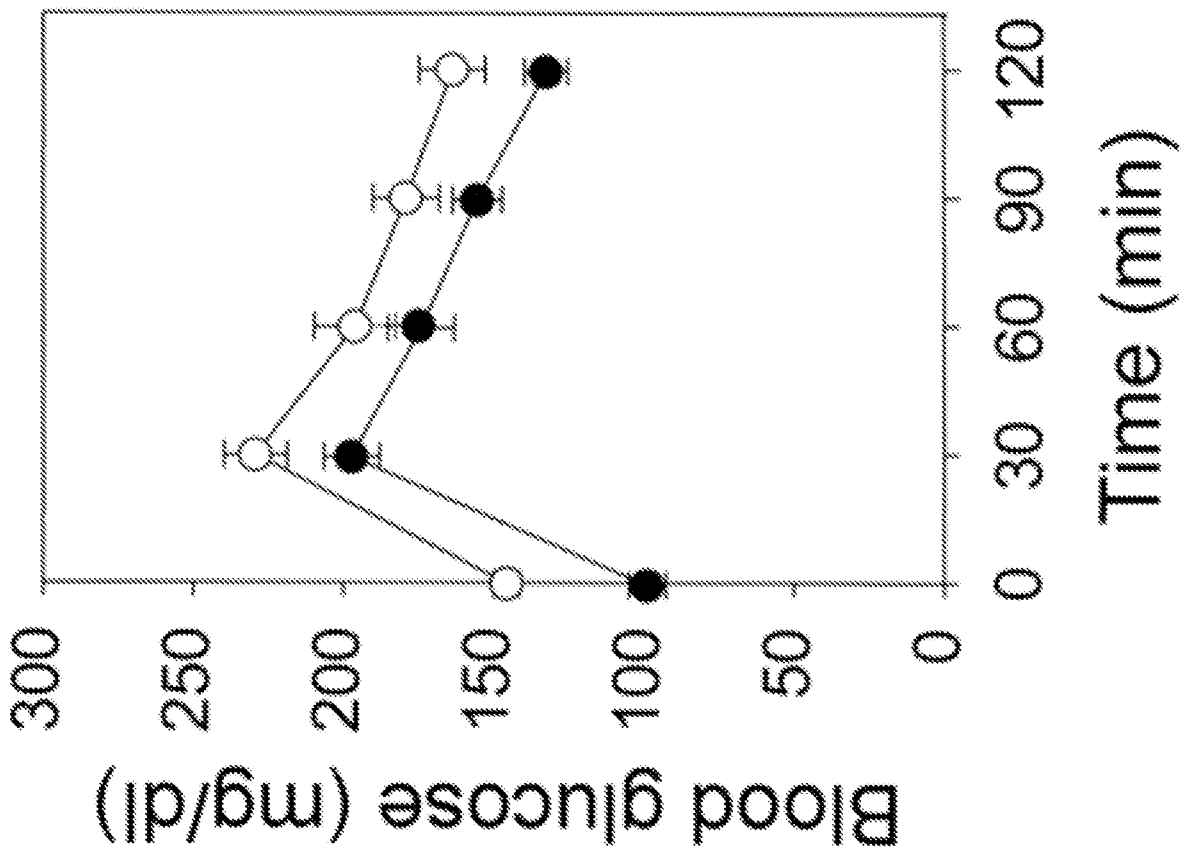

FIG. 13B

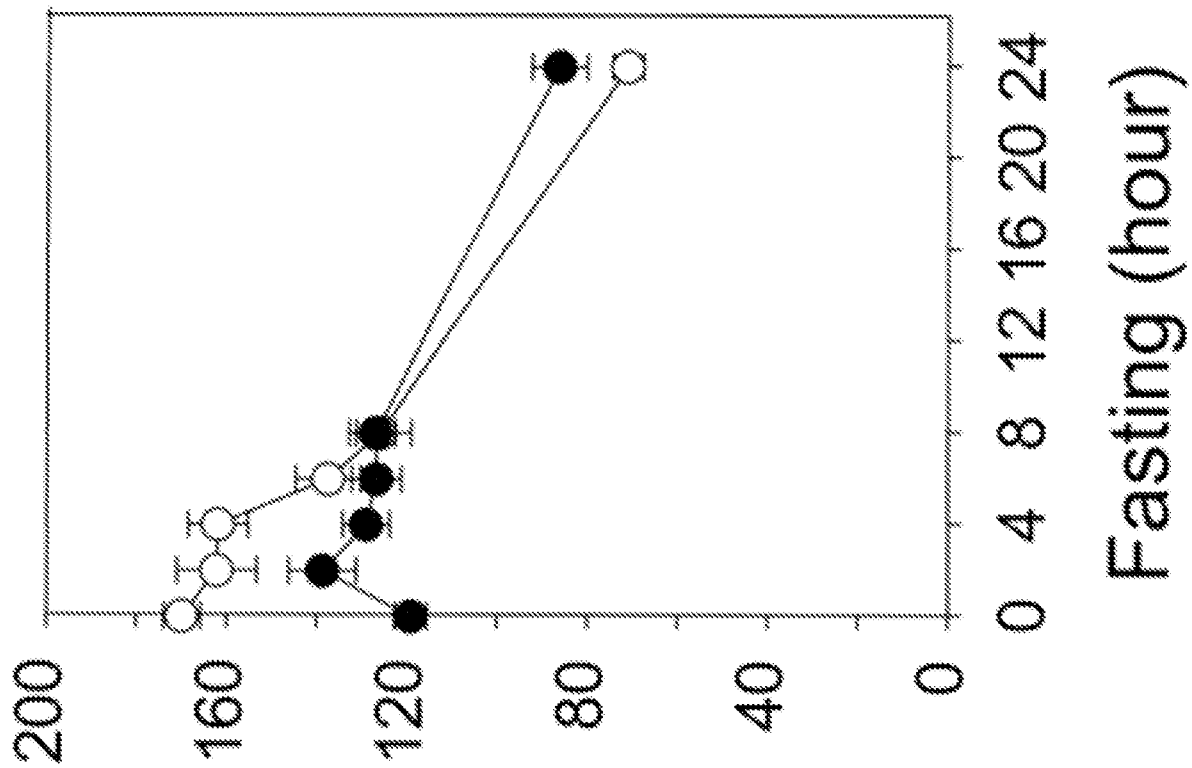

Hepatic G6Pase activity
(nmol/min/mg)
0
20
40
60
80
100
120
140
160
Age
4W
12W
GPE-G6Pase
GPE-Co-G6Pase
GPE-G6Pase
GPE-Co-G6Pase